applied sciences

MDPI

Review

State-of-the-Art of Colloidal Silica-Based Soil Liquefaction Mitigation: An Emerging Technique for Ground Improvement

Mingzhi Zhao [1,2], Gang Liu [1,2,*], Chong Zhang [1,2], Wenbo Guo [1,2] and Qiang Luo [3]

[1] School of Civil Engineering, Architecture and Environment, Xihua University, Chengdu 610039, China; 1220180013@mail.xhu.edu.cn (M.Z.); civilzhangchong@163.com (C.Z.); civilguowenbo@163.com (W.G.)
[2] Institute of Geotechnical Engineering, Xihua University, Chengdu 610039, China
[3] MOE Key Laboratory of High-speed Railway Engineering, Southwest Jiaotong University, Chengdu 610031, China; LQrock@home.swjtu.edu.cn
* Correspondence: 0120130047@mail.xhu.edu.cn

Received: 21 November 2019; Accepted: 29 November 2019; Published: 18 December 2019

Abstract: In the booming field of nanotechnology, colloidal silica (CS) has been introduced for ground improvement and liquefaction mitigation. It possesses a great ability to restrain pore pressure generation during seismic events by using an innovative stabilization technique, with the advantages of being a cost-effective, low disturbance, and environmentally friendly method. This paper firstly introduces molecular structures and some physical properties of CS, which are of great importance in the practical application of CS. Then, evidence that can justify the feasibility of CS transport in loose sand layers is demonstrated, summarizing the crucial factors that determine the rate of CS delivery. Thereafter, four chemical and physical methods that can examine the grouting quality are summed and appraised. Silica content and chloride ion concentration are two effective indicators recommended in this paper to judge CS converge. Finally, the evidence from the elemental tests, model tests, and field tests is reviewed in order to demonstrate CS's ability to inhibit pore water pressure and lower liquefaction risk. Based on the conclusions drawn in previous literature, this paper refines the concept of CS concentration and curing time being the two dominant factors that determine the strengthening effect. The objective of this work is to review CS treatment methodologies and emphasize the critical factors that influence both CS delivery and the ground improving effect. Besides, it also aims to provide references for optimizing the approaches of CS transport and promoting its responsible use in mitigating liquefaction.

Keywords: liquefaction mitigation; colloidal silica; transport mechanism; grouting material

1. Introduction

In the past few decades, large destructive earthquakes, such as the 1964 Niigata earthquake in Japan, the 1964 Alaskan earthquake, the 1985 Michoacán earthquake in Mexico, the 1995 Hyogoken-Nambu earthquake in Kobe, Japan, the 2008 Wenchuan earthquake in China, the 2010 Chile earthquake, and the 2011 Great East Japan earthquake, have resulted in various geological hazards in which liquefaction was particularly remarkable [1–6]. The 1976 Tangshan earthquake in China induced serious liquefaction in a vast area of 24,000 square meters. In the liquefaction area, the ground suffered a rapid and dramatic loss of soil strength, and the bearing capacity suddenly disappeared due to the motion of the earthquake, leading to the significant settlement or collapse of massive buildings. Liquefaction is a kind of natural hazard that usually occurs in loose, saturated sand during an earthquake. Under the effect of a vibrating load, sand particles deviate from their original location, separating from each other and becoming suspended in the pore water. Both dead seismic loads can only act on the pore water under

this circumstance, and the lateral movement of intact soil blocks over shallow liquefied deposits is typically induced. Some sloping areas in mountainous regions and those along the waterfront are more susceptible to lateral movement compared with the flat terrain. Therefore, the infrastructure in these areas is presented with a great risk from lateral spreading due to liquefaction [7]. Liquefaction-induced lateral spreading and ground failure will bring great damage to the upper parts of structures, which is a costly natural phenomenon. For example, a major part of the billion-dollar damage in the 1964 Niigata earthquake can be attributed to the lateral movement triggered by liquefaction. Besides, liquefaction also caused billions of dollars of damage to port facilities during the 1995 Kobe event [8,9].

To increase liquefaction resistance and limit the potential deformations of ground soil, one of the most popular soil improvement techniques is densification. Dynamic compaction, vibro-compaction, and explosive compaction have been extensively adopted to densify soil to mitigate liquefaction risk. Pioneering works, conducted by Dappolonia et al. (1954), Menard and Broise (1975), Mayne et al. (1984), and Welsh (1986), have facilitated the development and implementation of these densification techniques [10–13]. However, these reinforcement measures can only be adopted in undeveloped sites, given the fact that the buildings and structures are sensitive to vibration and dynamic compaction. At constrained and developed sites, underpinning and grouting seems to be the most feasible technique [7]. With underpinning, foundation is extended in depth or breadth so that it can either rest on a more supportive soil stratum or distribute its load across a broader area. The stress states of the existing structural elements are significantly improved in order to mitigate liquefaction. Nevertheless, this method targets specific structures rather than the entire ground. In the case of grouting, permeation grout can be classified into two categories, namely, cement suspension and chemically based solutions [14]. Both grouting materials are of high viscosity, so that they are often adopted to form grout columns rather than a uniform distribution across the entire ground beneath the structure [7,15]. In addition, most typical chemical solutions, such as acrylate and epoxy, are toxic and likely to create pollution to the local underground water. Especially in the case of cement, where the mean particle size of Portland cement ranges from 10–30 μm, allowing it to permeate through voids with a size greater than 0.2–0.3 mm. As a consequence, only on the condition that the soil stratum is mainly composed of medium to coarse sand can Portland cement be adopted as a grouting material. This is even the case with ultra-fine cement, where the mean grain size decreases to 3–5 μm, which has been proposed to be used in pressure grouting in recent years. Even this cement is only appropriate for use in fine to medium sand. However, liquefaction is more likely to occur when the stratum is mainly composed of silty sand or fine sand [16,17], so there are some limitations when using these traditional materials to mitigate liquefaction risk.

With the development of nanotechnology, nanomaterials have been proposed by many researchers to be introduced into ground treatment to improve mechanical properties and mitigate liquefaction risk [18–25]. The concepts and inspirations of nanotechnology originate from a famous talk hold by Richard Feynman entitled “There’s Plenty of Room at the Bottom” at Caltech, in Pasadena, California, in December of 1959 [26]. Since then, a new field, exploring and manipulating nanoscale microscopic particle has begun to develop at a breathtaking pace. At present, the economic benefit created by nanomaterials and relevant products annually increases by 20%. Meanwhile, the cost of nanoproduction decreases significantly with the promoting effect of booming market development [15]. Under these circumstances, nanomaterials, such as carbon nanotubes, nanoalumina, colloidal silica, nanobentonite, laponite, and so on, have an expansive application space in civil engineering, especially as kinds of additives to improve the properties of cement, concrete and soils [27–29].

Among these advanced nanomaterials, the cheapest and most widely used one in soil treatment is colloidal silica (CS) [30,31]. CS is a kind of powerful material that can be used for passive site stabilization, which is a relatively new technique that has been proposed by Gallagher (2002) as a nondisruptive treatment to mitigate liquefaction risk [32]. The passive site stabilization technique involves three critical procedures, namely, the injection of grouting materials at the upgradient edge of the site, the delivery of the stabilizing materials to the targeted location, and gelation into a rigid gel

(Figure 1). The most critical point in passive site stabilization is the smooth delivery of the grouting materials, with the condition of low-gradient terrain. Here, it is required that the given material in use has a low initial viscosity and excellent permeability characteristics, which it needs to sustain for sufficient time such that the modifier could be transported to the desired location [32,33]. Since CS has an extremely low initial viscosity of around 2 cP (where, as a comparison, pure water has an initial viscosity of 1 cP), after mixing with a salt solution, it can easily flow through the voids of liquefiable soil and permeate across the soil stratum, along with the underground water flow induced by the extraction wells [32]. Once CS reaches the target location, extraction is eliminated, waiting for the CS grouting gel to change into a firm solid. CS has been investigated by many scholars as a kind of grouting material for soil improvement and liquefaction mitigation. The mechanical behavior of the soil stabilized with CS has been evaluated in conventional geotechnical tests, bench-scale model tests and field tests [17–19,32–37]. It has been proven that CS can decrease the axial strain and restrain pore pressure development in the soil subjected to cyclic loading. Therefore, it is potential material to be adopted in ground treatment, especially for strata mainly composed of liquefiable soils.

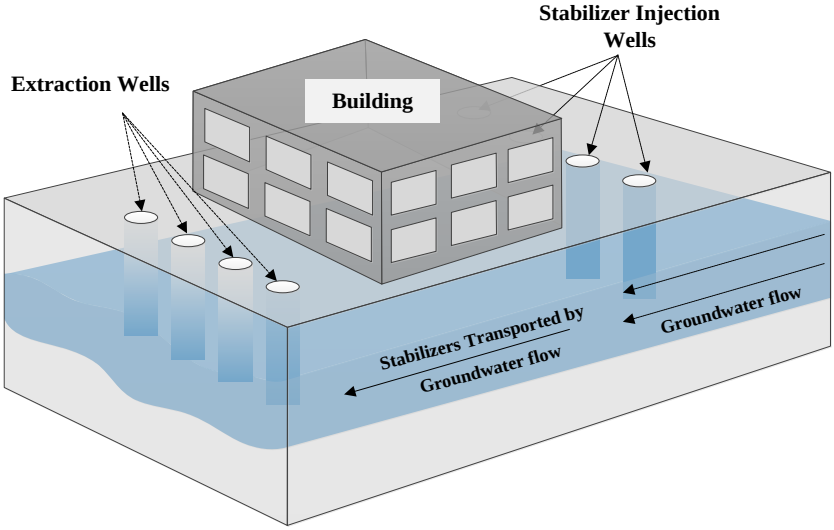

Figure 1. Concept for passive site stabilization [7,32].

The paper reviews the main experimental studies and scientific findings in the field of the applied research of colloidal silica for soil improvement and liquefaction mitigation. The paper is organized as follows: The first section describes the physical, gelling, curing, and mechanical properties of CS. The effect of ionic strength and pH on the gelation process are both discussed in detail. The paper then focuses on the mechanism of CS transport. Here, soil type, CS viscosity, and injection rate are summarized as three main factors that determine grouting quality and CS coverage. Thereafter, evidence from laboratory tests and field tests is presented to demonstrate the potential ability of CS in inhibiting pore water generation and decreasing dynamic strain. Finally, in the last section, the paper reviews further CS applications in other branches of civil engineering and sums some significant advantages of this innovative technique compared with traditional methods.

2. Characteristics of Colloidal Silica (CS)

2.1. Physical Properties of CS

Colloidal silica (CS) is an aqueous suspension of microscopic nanosilica, extracted from saturated solutions of silicic acid. In general, the particle size of nanosilica is uniform, ranging from 7–22 nm. CS is nontoxic, chemically and biologically inert, and environmentally friendly [38,39]. When diluted to a 5% concentration by weight, the viscosity of CS solution is only 1.5–2 cP, and is quite similar to

pure water. With the addition of an electrolyte, a CS solution can be destabilized in order to start the gelation process.

CS nanoparticles are formed as a result of the interaction between H_4SiO_4 and other molecules. During the manufacturing process, alkaline solutions are added into the CS to keep the silica particles ionized and repelled from each other, so that gelation can be inhibited, and the CS solution can stay steady [7]. The surfaces of the CS particles are initially distributed by uncombined silanol (Si-O-H) groups. When exposed to an alkaline environment, the alkali materials react with the surfaces of nanoparticles, leading to negative charges (O^-) on the particles and resulting in repulsive forces (Figure 2a). As the amount of charge on particle surfaces is proportional to the amount of hydroxyl ions, interparticle repulsive force weakens and particles start to interact with each other when the pH drops to a relatively low value. Under this circumstance, some of the silica particles still have negative charges (O^-), while the others become uncharged (–OH). Here, siloxane bonds (Si-O-Si) start to develop (Figure 2b) and the gelation of the CS suspension is motivated (Figure 3). As the pH drops continuously below 5, positive charges attach to the silica particles, and repulsive forces dominate once again (Figure 2c). Therefore, the gelation time increases with a decreasing formation rate of siloxane bonds. It has been investigated and determined that the minimum gelation time can be obtained when the pH ranges from 5 to 7 [40–42].

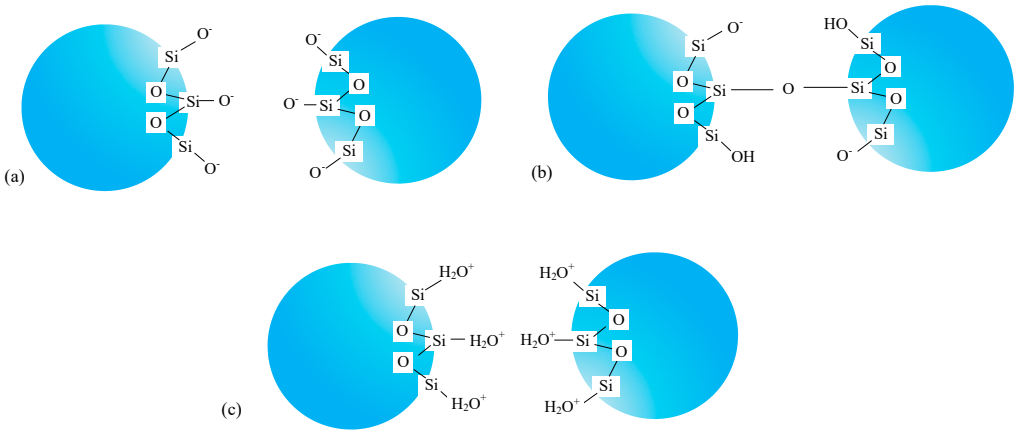

Figure 2. Surface charge characteristics of silica particles on the condition of different pH values: (**a**) pH > 8, O^- on the particle surface and repulsive forces demonstrated; (**b**) 5 ≤ pH ≤ 8, some particles still with O^- and others become uncharged; (**c**) pH > 8, H_2O^+ on the particle surface and repulsive forces indicated [7].

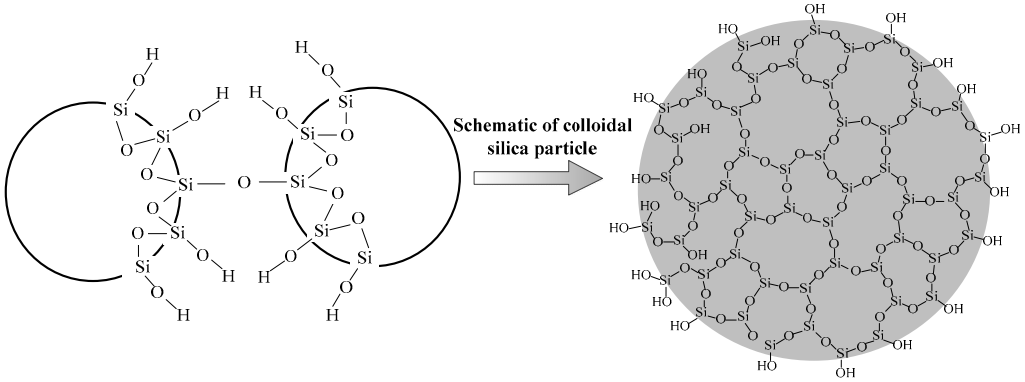

Figure 3. Formation of siloxane bonds and a schematic of the colloidal silica (CS) particle [40,43,44].

In addition to pH, the critical factors that could influence gelation process also include the ionic strength, silica solids concentration, and temperature [7,36,45,46]. Since silica concentration and temperature are relatively constant, gelation time can be controlled by adjusting the ionic strength

and pH value. The evolvement characteristics of viscosity in the gelation process for solutions with 5 wt % colloidal silica have been measured and depicted quantitatively [7,40,45], as shown in Figure 4. It is obvious that the shape of gelation curve is similar regardless of gel time. Moreover, silica particles have an induction period in the gelation process, during which viscosity stays fairly low and silica suspension has a flow rate close to pure water. With an appropriate amount of time elapsed, viscosity starts to increase dramatically, and a firm gel is finally obtained [47,48]. In detail, gel time increases with pH value on the condition of pH > 7.5, while it decreases as normality (i.e., ionic strength) rises from 0.225 N to 0.3 N. As a consequence, the time from mixing to the point where viscosity increases has a significantly wide scope, ranging from a few minutes to several months. In other words, CS has a widely ranged controllable gel time, which is favorable for the transportation of grouting materials to the desired location.

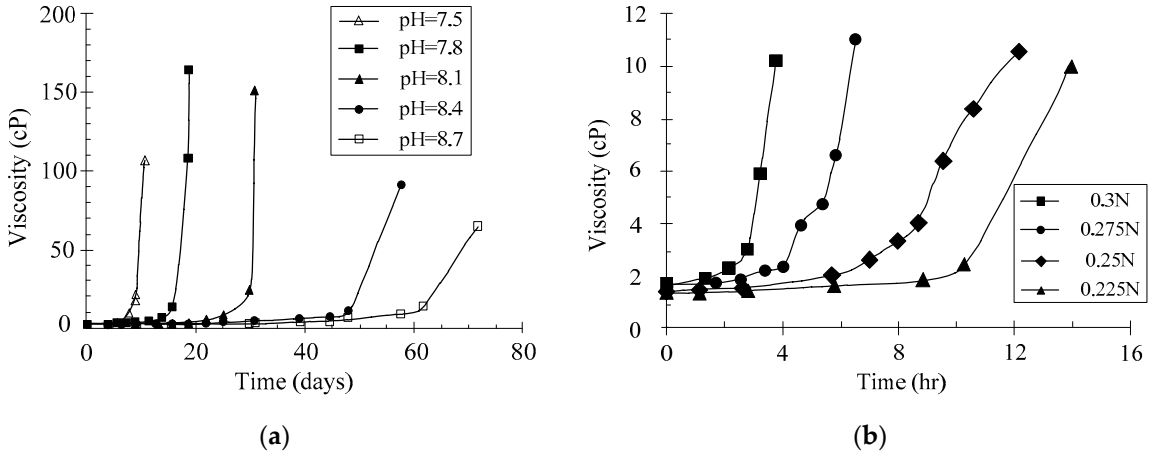

Figure 4. Viscosity increasing law of CS suspension in the gelation process at different (**a**) pH values and (**b**) ionic normalities [40,45].

2.2. Gelling and Curing Process for CS

Persoff (1999) divided the gelation process into 11 gel states to describe the course during which a CS solution evolves into a rigid gel [49], as shown in Figure 5. Gel state 1 is such a process, where an original CS solution has a viscosity quite close to pure water and no detectable formed gel. During this stage, CS acts like a Newtonian fluid. When the pH or salt concentration is adjusted, the gelation process is triggered, and CS enters into gel state 2. Here, viscosity increasing gradually, and the gel becomes a non-Newtonian fluid. Since then, CS transforms from a flowing gel into a nonflowing gel, and finally into a rigid gel. When arriving at gel state 10, CS particles gel into chainlike structures and then into uniform three dimensional networks. As a result, a CS resonating, rigid gel can be obtained. Therefore, gel time can be defined as the time needed for a CS solution to evolve from gel state 1 to gel state 10 [40,45].

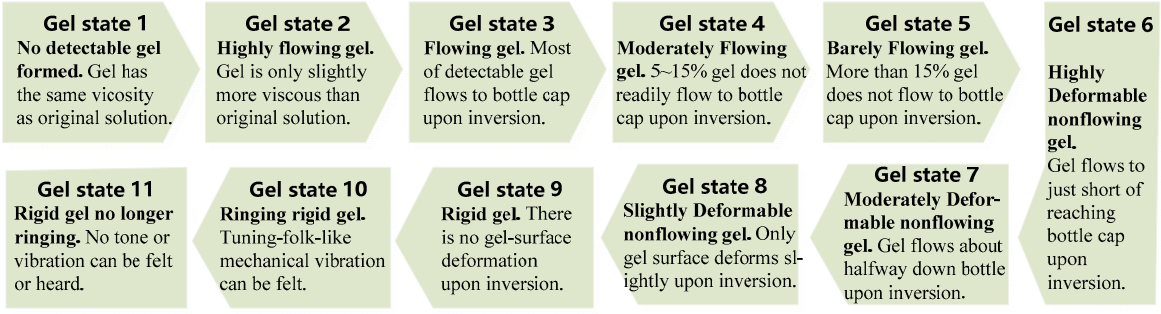

Figure 5. Gel state classification and description [49].

Since the relationship of gel time with pH value is not as clear as that with ionic strength, the salt concentration has always been adjusted to control the gel time in previous experimental studies in the literature [14,17,20,32,50]. Sodium chloride (NaCl) or calcium chloride ($CaCl_2$) has mostly been adopted as the electrolyte solution of choice to adjust salt concentration in order to start the gelation process. The addition of salt will shrink the double layer of CS particles, which will increase the probability of interparticle collisions [45]. These collisions will undoubtedly the motivate gel formation process and facilitate the CS suspension to transform into a rigid, firm gel. With NaCl addition to adjust the salt concentration, the CS gelling process was monitored by Wong et al. (2018), as shown in Figure 6.

(**a**) (**b**) (**c**)

Figure 6. CS gelation process: (**a**) before gelling; (**b**) close to gelling; (**c**) after gelling [50].

Mollamahmutoglu and Yilmaz (2010) performed a series of gel experiments with different salt concentrations and salt solution quantities, and the gel time curves for three magnitudes of salt concentrations were plotted against the addition quantities of the salt solution. It was concluded that gel time decreases with an increasing salt concentration and an increasing ratio of salt solution volume to CS volume [14]. Wong proposed that a 1.7 mol/L NaCl solution should be hand mixed with CS in a 1:5 ratio by volume to obtain a 1 h gel formation time [50]. The required salt concentrations to obtain the targeted gel time can be determined with the analytical model proposed by Pedrotti et al. (2017) [51].

Upon rigid gel formation, the gelation process is accomplished, and the curing period begins. The curing time is the time from where gel formation has finished to strength testing starts. It has been verified that curing time has a significant effect on the strength properties of a CS-soil mixture. Wong et al. (2018) investigated the influence of curing time and curing conditions on the strength properties of CS specimens. Four CS samples were placed under de-aired water to cure for 1, 2, 4, and 8 weeks after gelation was accomplished. At the same time, another CS sample was cured for 1 week at 90% relative humidity (RH). Oedometer tests were performed on the five samples, and the corresponding compression curves are shown in Figure 7. It can be seen in Figure 7a that the samples cured for 1 and 2 weeks had a single compression curve, while the samples cured for 4 and 8 weeks have another single (but different) compression curve. The samples cured for 4 and 8 weeks tended to have a stiffer behavior at low vertical stress. Figure 7b depicts that the sample cured at 90% relative humidity suffered some water loss during the curing period, leading to a lower initial void ratio compared with the specimens immersed in de-aired water. Moreover, the 90% RH sample showed a stiffer response than the immersed samples.

Persoff et al. (1999) measured the strength properties of CS-sand mixtures for a year and found that there is a continuously increasing strength gain during that period [49]. However, Gallagher and Lin (2005) found that strength gain only occurs during curing periods approximately four times as long as the gel time [45]. In any event, although a rigid gel is formed during the gelation process, the mechanical properties continuously develop during the curing process [52,53]. Therefore, both the curing time and curing condition have a significant impact on the strength behavior of a CS sample.

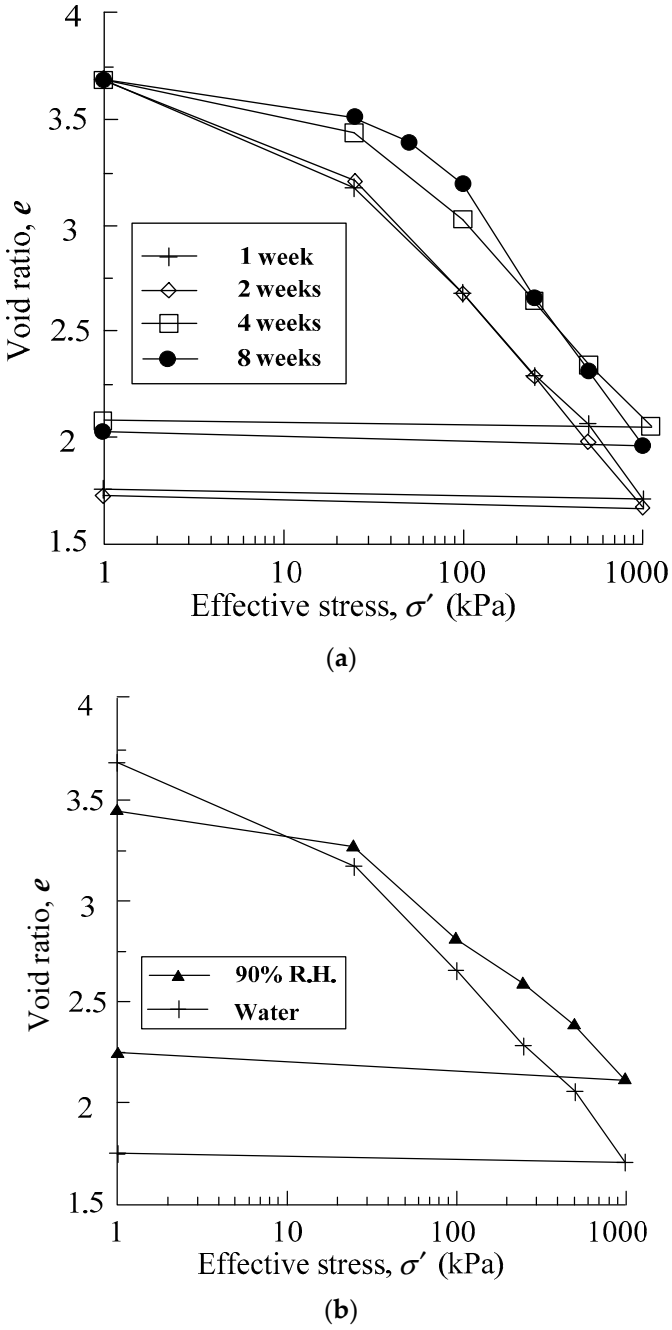

Figure 7. One-dimensional compression curves for CS samples: (**a**) Those cured with different durations; (**b**) those cured in different evaporation conditions [50].

2.3. Mechanical Properties of CS-Soil Mixtures

Once the gelling and curing process have been accomplished, some experiments can be performed on CS-soil samples to assess their static mechanical properties. Seyedi et al. (2013) studied the properties of a clay-lime mixture by performing CBR (California Bearing Ratio) tests and found that strength of the mixture increased by 2, 7.5, and 8 times when adding 1%, 3%, and 5% CS [54]. Yonekora and Mika (1993) observed a significant unconfined compressive strength gain for CS-treated sand samples compared to the original ones. They declared that the unconfined compressive strength reached 335 kPa when 32 wt % CS was grouted [18]. Moreover, the unconfined compressive strength of the treated sample was increased with the increased concentration of the CS additive [19,55], as shown in Figure 8. The increase in CS concentration will aid in intensifying the bonds between CS and soil

particles, thus developing a higher compressive strength. They further reported that the logarithm of hydraulic conductivity of the mixtures decreases almost linearly with the increase of CS concentration. The relationship between CS concentration and unconfined compressive strength, as well as hydraulic conductivity, has been recognized and summarized by Ghasabkolaei et al. (2017) [56]. Noll (1992) also reported the reduced hydraulic conductivity of loose sand when mixed with 5 wt % CS. It was interesting to find that the hydraulic conductivity reduced to 9×10^{-9} cm/s for the grouted sand sample [57].

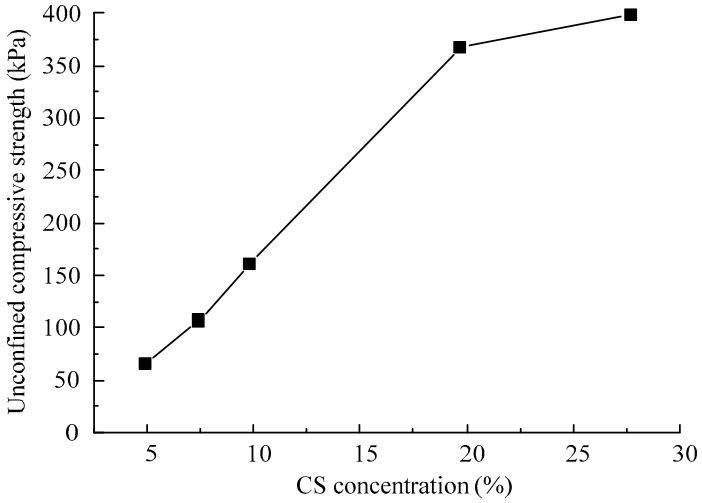

Figure 8. Relationship between unconfined compressive strength and CS concentration (data collected from Persoff et al.) [19].

Since soil samples grouted with CS will improve compressive strength, CS-soil mixtures should also obtain a higher shear strength compared with pure soil samples. Changizi and Haddad (2015) added 0.5%, 0.7% and 1% CS to soil to discover the mechanical enhancing effect. They found that both the friction angle and cohesion were enhanced for grouted soils [58]. Besides, the relationship between the shear stress ratio (the ratio of shear stress to effective vertical stress) and shear displacement was investigated for a pure sand sample, a 1-week-cured CS-sand sample, and a 4-week-cured CS-sand sample, as shown in Figure 9 [50]. In the conditions where the effective vertical stress equaled 100 kPa, 200 kPa, and 300 kPa, all of the grouted sand samples had a higher peak stress when compared with the untreated samples. Furthermore, the 4-week-cured CS-sand sample had a greater peak shear stress than the 1-week-cured sample when the vertical stress was 200 kPa. At an effective vertical stress of 100 kPa and 300 kPa, although the shear stresses of the grouted samples seem to share a similar peak value regardless of curing time, the sample cured for 4 weeks showed an initial stiffer response than the sample cured for 1 week. In summary, CS grouting can remarkably improve the static mechanical properties of sand samples. In this process, curing time is a main factor that determines the strengthening effect.

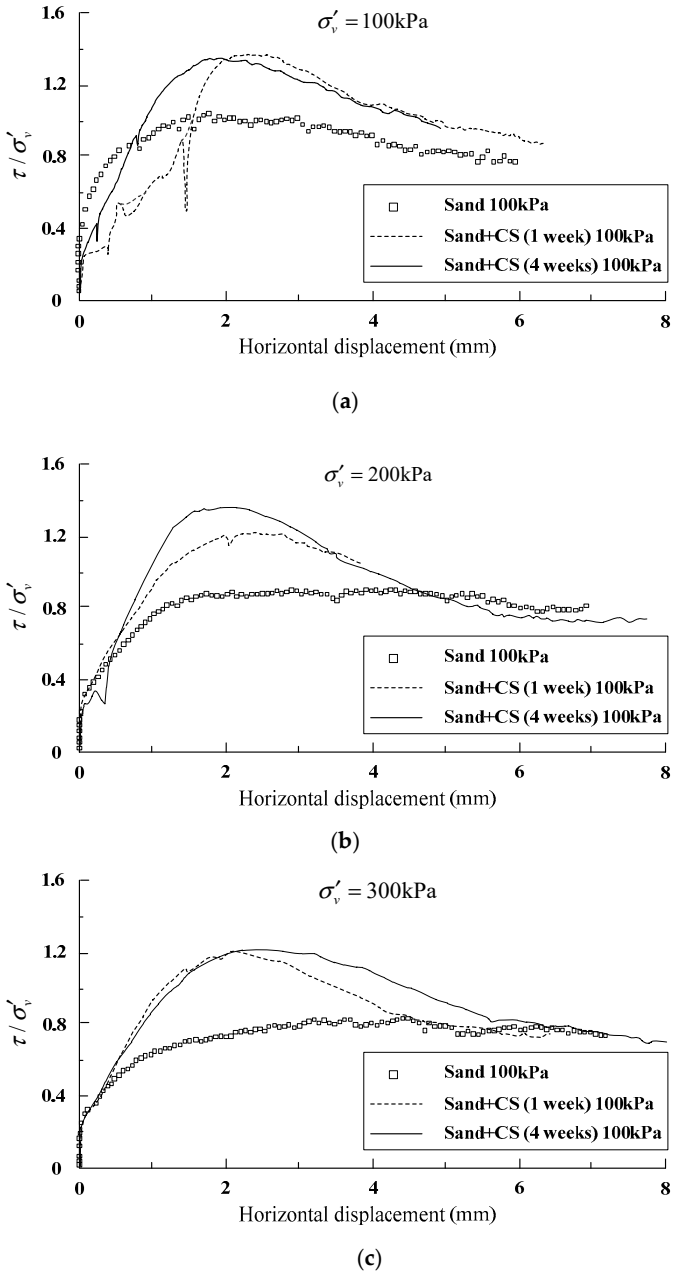

Figure 9. Horizontal displacement versus the ratio of shear stress to vertical stress for a pure sand sample and a sand sample grouted with CS under effective vertical stresses of (**a**) 100 kPa, (**b**) 200 kPa, and (**c**) 300 kPa [50].

3. Colloidal Silica Transport Through Soil Stratum

3.1. Feasibility of CS Transport Through Porous Media

The transport issue of CS is the most critical aspect, determining the feasibility of CS when adopted for ground improvement and liquefaction mitigation. Laboratory and field tests have indicated that colloids can potentially mobilize in aquifers [45], which provides direct evidence for CS transport in liquefiable soil layers. Ryan et al. (1999) investigated the permeability characteristics of a mixture of bacteriophage PRD1 (62 nm diameter) and CS (107 nm diameter) in sewage-contaminated and uncontaminated areas of an iron oxide-coated sand layer. Although attachment of the mixture to the porous media appeared initially, release occurred by adjusting the pH, adding an anionic surfactant to change the surface charge, and adding a reductant to dissolve the iron oxide coating on the particles.

The results demonstrate that the physicochemical properties of the porous media could be modified to facilitate the permeability of colloids [59]. Therefore, the transport of colloids in porous media is feasible with or without treatment of the soil stratum.

Higgo et al. (1993) monitored the permeable properties of CS in a kind of glacial sand by conducting a laboratory column test and field test. In the laboratory test, almost 100% of the silica particles could be transported in the porous media. However, only 70–80% CS particles mobilized over a distance of 1.6 m. The differences in these two tests could be due to the heterogeneity of the sand layer in the field compared with that in the column, but both tests provide evidence that CS particles can be delivered in a liquefiable sand layer to the targeted location with sufficient concentrations in order to stabilize the soil [60]. Saiers et al. (1994) proposed that a one-dimensional advection-dispersion equation could be adopted to model CS transport through nonreactive porous media, on the condition that a small amount of CS deposition occurred [61]. In engineering practice, CS will suffer various degrees of physical and chemical deposition due to the geochemical properties of the underground water and porous media. The deposition process can significantly delay the transport of CS [62]. However, Johnson et al. (1996) performed a series of short column tests to study the influence of ionic strength on the transportation of CS. He pointed out that CS deposition took place for chemically active sand media and was more obvious at a low ionic strength. Despite deposition occurring, full colloid concentration could be achieved at the desired location [63].

A box model was adopted by Gallagher et al. (2007) to study the feasibility of CS transport in liquefiable sand. The box was divided into three compartments, namely, a central chamber used for sand placement and two water reservoirs, located at both sides, for groundwater control [7]. The model was filled with Nevada sand, with relative density of 40%, to a height of 200 mm, as shown in Figure 10. Five injection wells constructed from 19-mm PVC pipes were arranged by pushing them into the sand deposit. Two extraction wells were set at the other side of the box model. The CS solution was colored with red food dye, so that the advancement of grout could be visually observed on the top and sides of the model. At the same time, the chloride concentration, which is a good indicator of the CS concentration, was measured in order to reflect the transport of CS grout. After CS transport was completed, the model was cured for 14 days. Then, six block samples were excavated and carved into smaller samples to perform unconfined compression tests with. It was indicated that the unconfined compressive strength ranged from 16 kPa to 61 kPa, which is quite close to the results reported by Gallagher and Mitchell (2002) [32]. Here, visual observation, chloride concentration measurement, and the unconfined compressive strength clarify that fairly uniform CS-sand mixtures were developed, which further demonstrate that CS could transported by a low-gradient stabilizer delivery. These findings indicate that the targeted place could be filled with CS at sufficient concentrations to stabilize the soil, even with physical and chemical deposition, which was unavoidable during the transport process, which would typically restrain the delivery of CS.

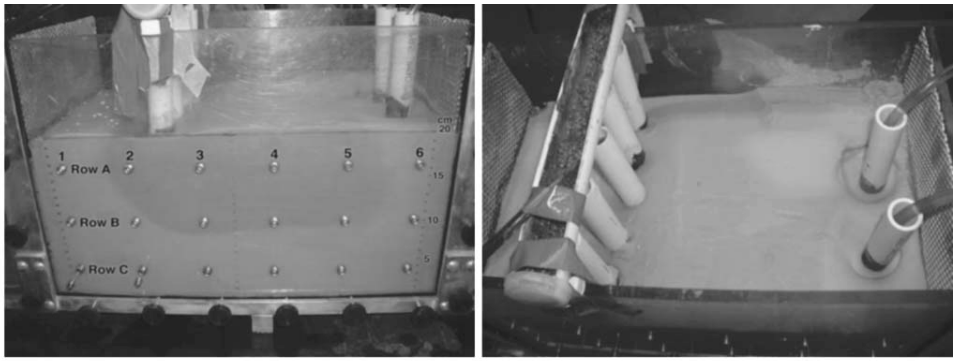

(a) Side view (b) Plan view

Figure 10. Photo of box model test [7].

3.2. Transport Mechanisms of CS in Liquefiable Sand

CS transport, which is a complicated physical process, is determined by several internal and external factors. Since CS has already been mixed with an electrolyte prior to injection, the transport of CS is significantly influenced by the time-dependent gelation process and is a more complicated course than a simple colloid transport. Previous to gelation, CS behaves like a Newtonian fluid. CS transport is quite similar to a simple colloid delivery. When gelation is motivated, CS becomes a non-Newtonian fluid. Viscosity increases continuously and gradually become the dominating factor that controls the transport of CS [49,64,65]. On the other hand, porous media with higher hydraulic conductivity presents larger porosity, which is more convenient for CS delivery than that with lower porosity (hydraulic conductivity). Therefore, viscosity and soil type are the fundamental internal factor that could influence CS transport. Moreover, some external factors, such as the injection rate, could also have a significant effect on the transport of CS. The influencing mechanisms of soil type, CS viscosity, and injection rate on CS delivery are reviewed and summarized as follows.

3.2.1. Soil Type

Gallagher and Lin (2009) designed a series of column tests to investigate the factors that could influence CS transport. The column used was made of a PVC pipe, with an internal diameter of 10 cm and a total length of 90 cm. Nevada and Ottawa sand, with hydraulic conductivities of 8.9×10^3 and 220×10^3 cm/s, respectively, were adopted as the porous media to fill in the column. The inlet water chamber was connected to the bottom end cap to supply steady water flow, as shown in Figure 11. CS grout (pH = 6.8, ionic strength = 0.1 N) was delivered through the valve located 5 cm above the bottom cap. During testing, water and CS were transported through the entire column to the outlet chamber. Nine sampling ports were set to obtain samples in order to study the influencing factors. The results show that the traveling time of the CS grout through Ottawa sand was two orders of magnitude lower than through the Nevada sand. It is worth noting that the hydraulic conductivity of Ottawa sand is two orders of magnitude higher than Nevada sand, which indicates that the hydraulic conductivity of the porous media used is significantly correlated with the delivery rate of CS grout.

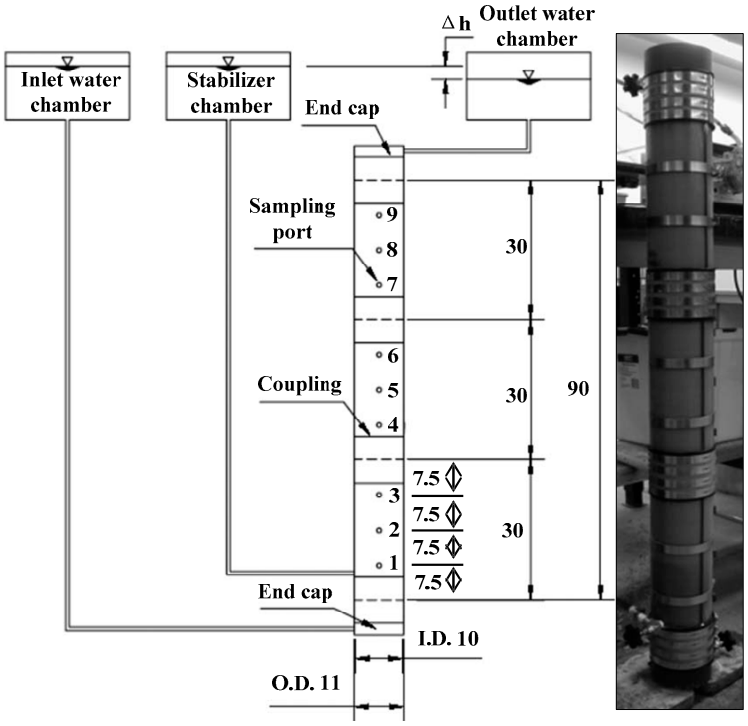

Figure 11. Schematic and photo of the column test [45].

3.2.2. CS Viscosity

With the increase of viscosity of the used colloid, the hydraulic conductivity of the porous media decreases synchronously. According to the Kozeny–Carman equation, the hydraulic conductivity of the porous media is inversely proportional to the viscosity of the permeant, as expressed by the following equation:

$$k = \frac{\kappa\gamma}{\mu} \quad (1)$$

where k is the hydraulic conductivity, κ is the intrinsic permeability, γ is the permeant density and μ is the permeant viscosity [45]. With a double increase of permeant viscosity during the transport, there is a double decrease in the hydraulic conductivity of the porous media, and there is a double decrease of flow rate under the same hydraulic gradient when substituting Equation (1) into Darcy's law. In summary, although CS can be transported though porous media (loose sand) with deposition and release, the viscosity of the permeant must be controlled to be as low as possible to facilitate the transportation of colloids.

Several permeation tests with different pH and ionic strengths have been performed using the column shown in Figure 11 to study CS transport mechanisms [45]. In these tests, the column was filled with Nevada sand by the pluviation method. It was indicated that the smoothest CS flow could be obtained when the pH was 6.5 and the ionic strength was 0.1 N. When pH was lowered to 6.2 or ionic strength was increased to 0.15 N, the CS gelled prematurely, and it was difficult to reach 100% coverage of the entire column. It should be noted that pH and ionic strength influences the viscosity, thus influencing the transport of CS. The flow rate of CS remarkably decreases as a result of the increase of viscosity in the source CS, which is quantitatively shown in Figure 12. Therefore, viscosity is the dominating factor that controls the flow rate and scope of CS in the column.

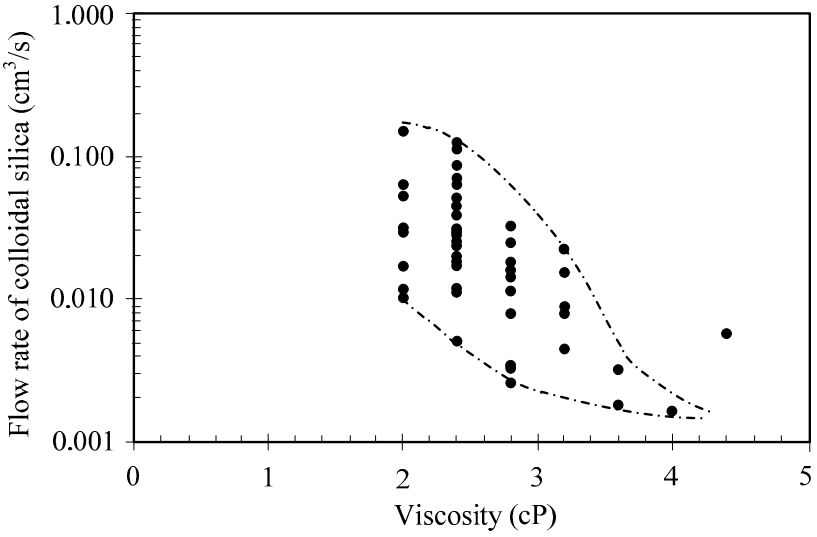

Figure 12. Relationship between flow rate of CS and viscosity [45].

3.2.3. Injection Rate

Conlee (2010) reported that CS has a tendency to sink downwards in a 9 m^2 field injection when the injection rate is less than 3700 mL/min/well [66]. Hamderi and Gallagher (2013) verified the sinking behavior of CS using anumerical method. They believe that the maximum transport distance for CS ranges from 2.5 m to 4 m due to the higher density of CS solutions compared with pore water [67,68]. To further investigate the sinking behavior and horizontal movement of CS grouting, they developed a 10 m^3 pilot-scale box model [69], as shown in Figure 13. The loose sand layer was placed in the box model by freely pouring sand onto water. Four injection wells and 4 extraction wells were set at the upstream and downstream sides, respectively. A constant head water flow was established, lasting for

7 days, saturating the sand layers prior to grouting. In low injection rate tests, injection rates of 65 and 130 mL/min/well were adopted to transport CS into the sand layers. However, CS was mainly present at the bottom of the model upon excavation, indicating that the CS sinking behavior is significant. When the injection rate increases above 1900 mL/min/well, sufficient horizontal pressure forces the CS grouting to horizontally move to the targeted location. Therefore, the transport of CS is more likely to be successful with a high injection rate. Since it is difficult for CS to permeate through porous media when the viscosity increases up to 4 cP [45], the gel time is expected to be appropriately controlled to meet the conditions where viscosity can increase beyond 4 cP to prevent gravitational sinking once the target location is reached.

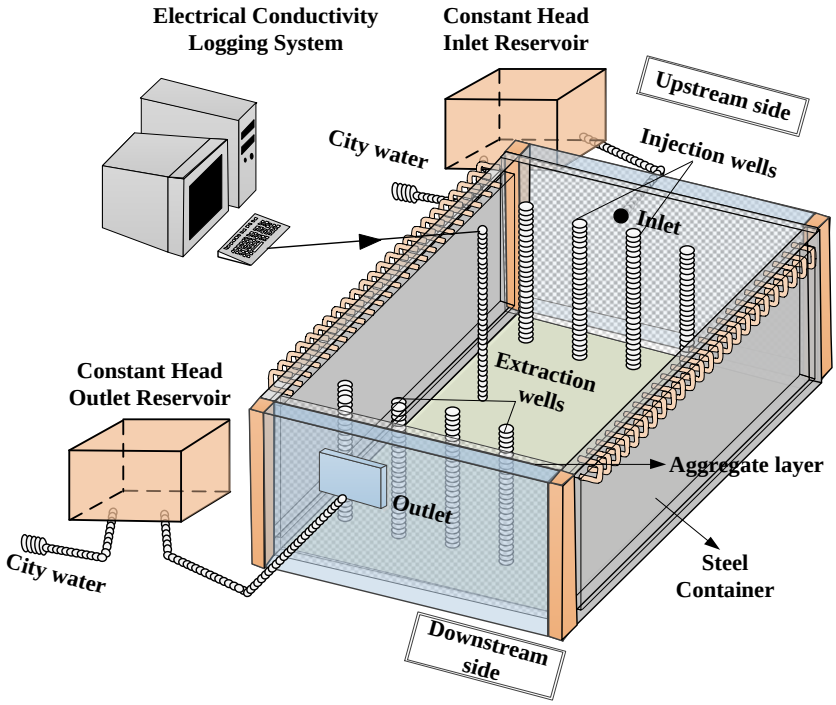

Figure 13. Setup of the pilot-scale model test to investigate the influence of injection rate (modified after Hamderi and Gallagher, 2015) [69].

3.3. Advancement for CS Transport

As stated above, CS grouting is conventionally implemented by injecting a stabilizer through a vertical injection well and consequent horizontal transport, where the underground water flow is motivated by the extraction well (Figure 1). The gel time of CS should be controlled to be sufficiently long, such that the CS viscosity stays below 4 cP during delivery. A low viscosity status should be sustained to facilitate CS horizontal transport. However, once CS arrives at the targeted location, sinking and deposition will occur on the condition of low viscosity [66–70]. Therefore, gel time is difficult to control in the conventional CS grouting method.

To settle this problem, Rasouli et al. (2016) reported a method where the delivering injection nozzle to the designated area uses a controlled curved drilling (CCD) machine [37], as shown in Figure 14. The new CCD machine used for CS grouting originates from the curved drilling machine that has been adopted in the oil industry [71,72]. The critical technology of a CCD machine is the curved drilling rod. To make such a curvature, the drilling head and water jet should firstly advance slantwise. At the location where the bore needs to be curved, the drilling head is inclined downwards and water is injected from the nozzle under a high pressure to push the drilling rod and the earth. As a consequence, an upward pressure is produced and applied on the inclined surface of drill head, finally creating a curvature along the boring path, as shown in Figure 15. Here, a CCD machine has

been adopted to transport CS to reduce the liquefaction potential of runways at Fukuoka International Airport in a seismic-retrofitting project. By using the CCD method, a CS grout with short gelation time is required. Post-treatment measurements show that the CCD method could be applied to inject CS to the loose sand layer to mitigate the liquefaction risk without disturbing the surface of the runways. In addition, the new grouting method could transport CS to the desired location directly, avoiding unnecessary attachment and deposition during the delivery process.

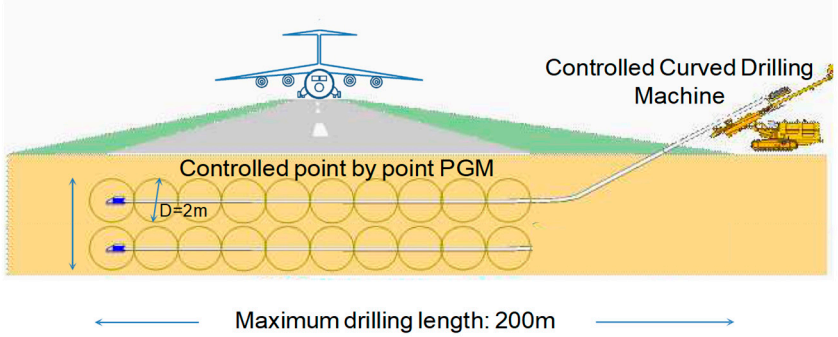

Figure 14. Controlled curved drilling (CCD) machine with the permeation grouting method (PGM) [37].

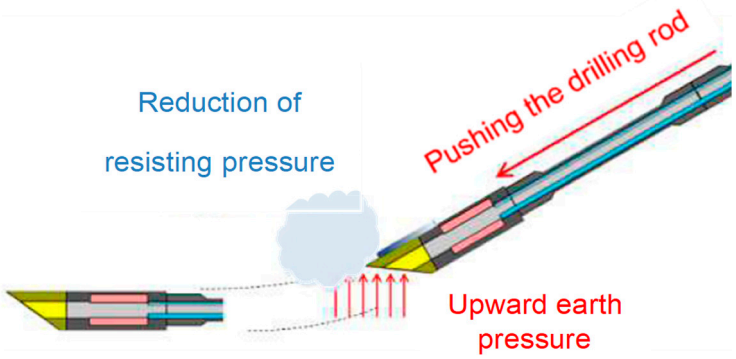

Figure 15. Mechanism for making a curvature [37].

3.4. Evaluation Method for CS Grouting Quality

After the injection and transport of CS in the liquefiable layer, the stabilizer should reach the desired location where improvement is needed. However, since the transport of CS is not always controllable, it is necessary to conduct a post-operation investigation to check the grouting quality. Several investigation methods have been reported in previous literature to evaluate the grouting quality, and these are detailed in the sections below.

3.4.1. Colored Tracer Chemical

Colored tracer chemicals can be grouted and transported with CS to provide a visual observation method to indicate the location where the stabilizer has arrived at. Generally, red food coloring and the methyl red indicator are selected as the tracer materials here [7,37,40,45]. Red food coloring is mostly adopted in the column test and centrifuge model test to reflect the grouting quality. The emerging grout in the model is very light in color when initially compared with the source grout, due to dilution via pore water. As the grouting process continues, new CS grout arrives at the location, and the grout becomes darker. At last, the grout is observed to present the same color as the source grout, indicating that the observed point is filled with CS at a full concentration. The methyl red indicator was used in the grouting project at Fukuoka International Airport. The working mechanism of the methyl red indicator is that it could present as red in color if the soil was treated with CS on the condition of acidic ground water. The CS grout used in this project had a pH of 3.5, leading to the soil becoming

weakly acidic. Therefore, the methyl indicator will become red at the location where CS treatment has occurred. Soon afterwards, samples can be extracted from the treated layer for visual observation, as shown in Figure 16.

Figure 16. Checking grout quality using the methyl red indicator [37].

3.4.2. Silica Content

Silica content is a direct indicator of CS. Gallagher and Lin (2009) proposed that the silica content of the pore fluid can be measured by burning a given volume of fluid at 200 °C for 2–3 days [45]. The weight of the material remaining after burning is considered as silica-containing material and can be used to calculate the silica content in the pore solution. However, some electrolyte solutions, such as NaCl or $CaCl_2$, may added in the solution to motivate the gelation process. Thus, the remaining material after burning also contains some other chemicals. Although Gallagher and Lin (2009) believed that the weights of the dissolved solids in the solution could be neglected when compared with the weight of the silica, the burning method may overestimate the silica content in the pore fluid, thus overestimating the grouting quality.

To avoid overestimation, Rasouli et al. (2016) suggested that the silica content can be measured by atomic absorption spectrometry (ABS) [37]. In this method, 100 mL of potassium hydroxide with a concentration of 20% is added for every 50 g of improved soil sample. Then, the mixture is heated in an oven at 120 °C for 30 min. Afterwards, 20 mL of supernatant liquid is collected to measure the silica content via the ABS method. Here, it was shown that the unconfined compression strength of the improved soil almost linearly increased with the silica content measured by the ABS method for the soils at the same sampling site, indicating that ABS is an appropriate approach to evaluate silica content.

3.4.3. Chloride Ion Concentration

Chloride ion concentration is much easier to obtain than CS concentration. An ion meter equipped with chloride probes can be used to detect the chloride concentration. Meanwhile, the coverage of CS grout can be evaluated by measuring chloride ion concentrations in the pore fluid. It has been verified that the normalized CS concentration is proportional to the normalized chloride concentration, as shown in Figure 17 [45]. The normalized concentration refers to the concentration calculated by dividing the sample concentration to the source solution concentration. This result indicates that chloride concentration is a precise indicator for CS concentration. Cl^- concentration has been adopted to monitor CS transport and coverage in other previous works [7].

3.4.4. Unconfined Compression Strength

A rudimentary unconfined compression strength was adopted by many researchers to evaluate the grouting quality and degree of stabilization achieved [7,14,37,45]. It has been widely acknowledged that the unconfined compression strength is positively correlated with the cyclic strength for both liquefiable and improved soils. Since the unconfined compression test is easier to operate and handle, it has been adopted as an index indicator test to reflect the cyclic strength of the targeted soil specimen and further evaluate the coverage of CS grout. In addition, when larger particles exist in soil

samples, the unconfined compression strength is difficult to obtain with an unconfined test. In this instance, an unconsolidated undrained (UU) triaxial test can be used to obtain the Mohr's stress circle. Then, the shear strength can be deduced from the failure line and finally the unconfined compression strength can be calculated by multiplying the shear strength by 2 [37].

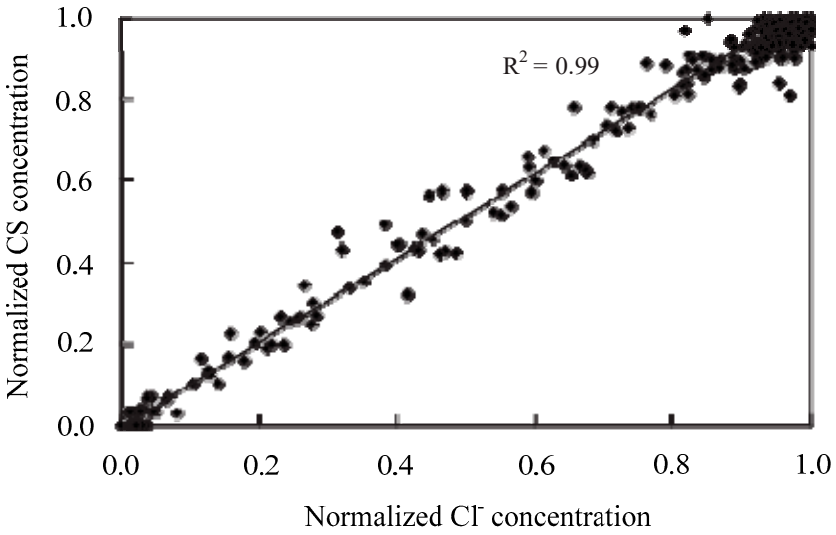

Figure 17. Relationship between chloride ions and silica concentration [45].

In summary, four methods, including the colored tracer chemical method, the silica content method, the chloride concentration method, and the unconfined compression strength method, were proposed in the previous literature to evaluate the coverage of CS grout and to make judgements concerning grouting quality. The colored tracer chemical method is the most simple and direct method, by which visual judgement can be conducted by color variation in the grouting process. However, CS concentration and grouting quality at a given place cannot be evaluated quantitatively with this method. The unconfined compression strength method can be applied to evaluate the grouting quality properly and quantitatively, however, the mechanical test, which is more complicated than the physical index test, needs to be performed here. Silica content and chloride concentration can be measured quantitatively by a simple physical index test, and they are perfect indicators of CS coverage. Therefore, the silica content method and chloride concentration method have been mostly adopted in experiments and practices to judge grouting quality.

4. Liquefaction Mitigation Using Colloidal Silica Grout

4.1. Dynamic Properties of CS-Soil Mixture

CS is an excellent additive for liquefiable loose sand to improve its liquefaction mitigation ability. When CS is properly grouted, cementation occurs between sand particles due to the presence of CS, and thus, loose sand layers tend to have a stronger cyclic resistance, avoiding liquefaction during an earthquake event. Clough et al. (1989) investigated the influence of cementation on the dynamic properties of liquefiable sands. They believed that loose, cemented sand tend to have a similar behavior to dense, uncemented sands. Moreover, liquefaction resistance increases as the degree of cementation increases [73]. Towhata and Kabashima (2001) performed a triaxial test on a 5 wt % CS-grouted sand sample and found that the non-deformability of a loose sand sample at 40% relative density is similar to that of the same kind of sand sample at 75% relative density after being mixed with 5% CS [74]. Rodriguez and Izarraras studied the reduction of liquefaction risk for loose sand treated with CS. They pointed out that grouting with 15 wt % CS would significantly improve the dynamic resistance against liquefaction [75].

To evaluate the liquefaction resistance quantitatively, Gallagher and Mitchell (2002) performed triaxial tests on pure Monterey sand and Monterey sand treated with CS [32]. The axial strain during the tests was recorded and is shown in Figure 18. Although very little strain was observed prior to liquefaction for the untreated sample, large strains occurred rapidly once liquefaction was motivated. The sample, tested at a cyclic stress ratio CSR of 0.27, could only suffer 13 cycles before it thoroughly collapsed. Furthermore, 5% double amplitude axial strain was produced in 12 cycles. However, the sample treated with 10 wt % CS experienced much less strain during cyclic loading. The treated sample required 276 cycles to reach 5% strain. Since a magnitude 7.5 earthquake was deduced to generate 15 uniform stress cycles [76], the 10% CS-treated sample could be expected to have a sufficient ability to resist liquefaction in such an earthquake event.

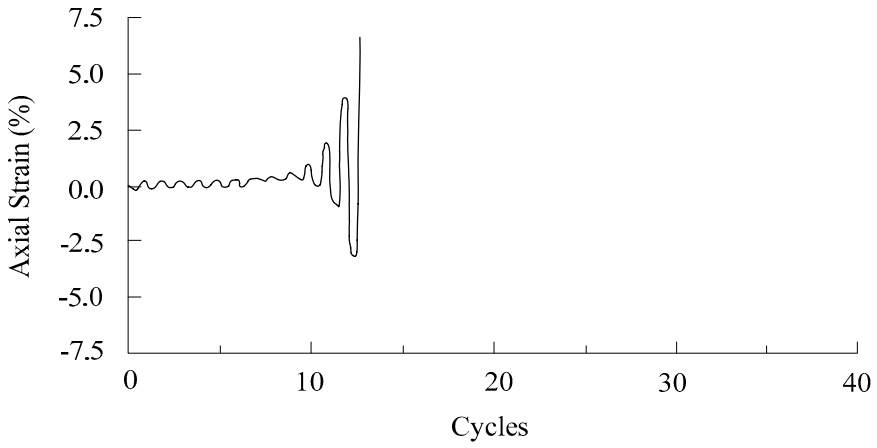

(**a**) Untreated sample

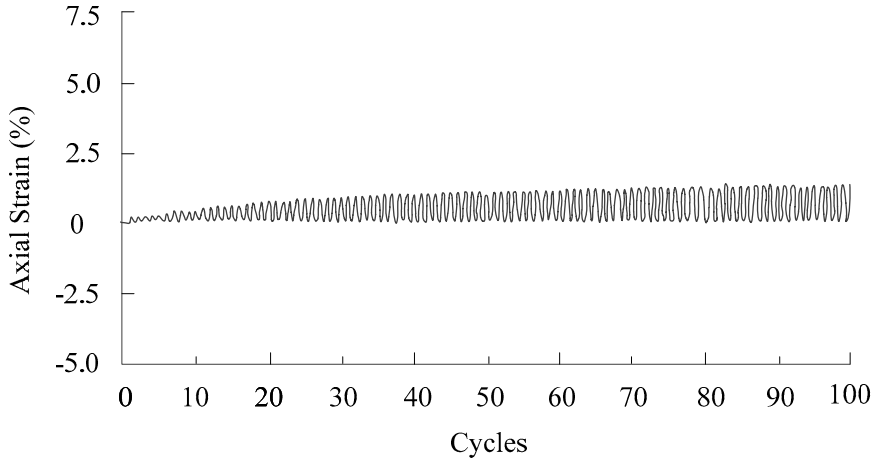

(**b**) 10% CS-treated sample

Figure 18. Axial strain during cyclic loading for both the untreated and treated samples [32].

Apart from the triaxial test, other laboratory element tests, such as the cyclic torsional shear test, resonant column test, and cyclic simple shear test, were also performed to investigate the dynamic properties of the CS-soil mixture. Ann undrained hollow cylinder torsional shear test was performed by Kodaka et al. (2005) on both CS-treated and untreated soil samples [77]. For the untreated sample, the cyclic stress ratio was set to be 0.23, and large strains occurred rapidly with a few additional cycles after arriving at phase transformation line. However, the CS-treated sample had a cyclic stress ratio of 0.60 and presented much less shear strain during the cyclic loading process (Figure 19). In fact, collapse and liquefaction did not occur in the whole cyclic loading process for the treated sample.

Spencer et al. (2008) conducted resonant column tests on pure Nevada sand and Nevada sand treated with two different concentrations of CS [41]. They found that the CS-sand mixtures had a slightly higher shear modulus than the untreated sample. Besides, an increase of 6 MPa in the shear modulus was observed for the sample treated with a 5% concentration of CS after a curing period of 28 days. However, the grouting of CS had little effect on the damping ratio for Nevada sand.

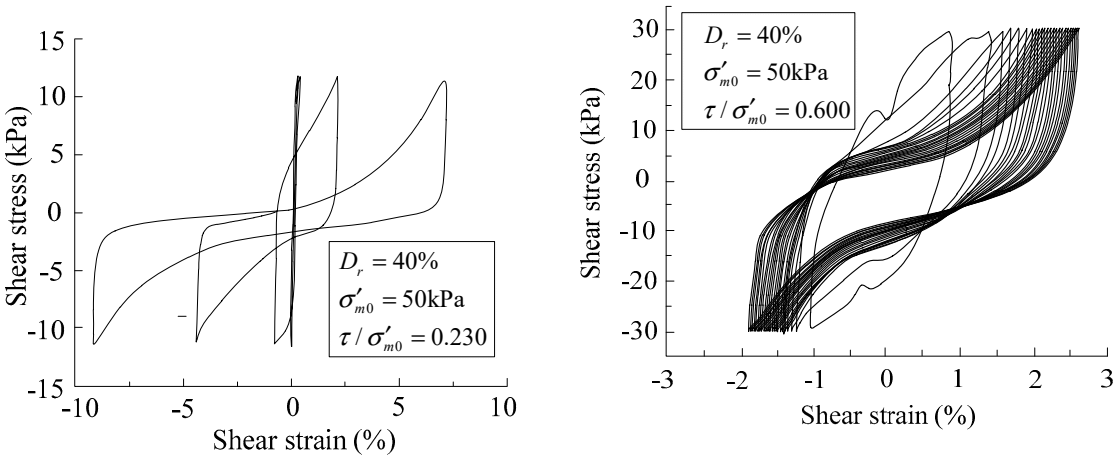

(**a**) Untreated sample (**b**) Treated sample

Figure 19. Shear strain of the untreated and treated soil samples in an undrained cyclic torsional shear test [77].

In addition, Díaz-Rodríguez et al. (2008) investigated the dynamic behaviors of sand samples grouted with CS in more detail through a simple shear test [17]. The required cycles to reach a 5% double amplitude (DA) shear strain were recorded for both the untreated and CS-treated samples at 40% and 60% relative density (Figure 20). It is remarkable that the CS-treated samples need more cycles to reach 5% DA strain than the untreated samples under different effective vertical stresses, which was the case for both of the samples with 40% and 60% relative densities. Furthermore, the required cycles to reach liquefaction increased significantly with the increase of CS concentration. Taking a 5% DA shear strain as the label of onset of liquefaction, when the CS concentration ranges from 0% to 14.5%, the required cycles to initiate liquefaction remarkably increase from 2 to 17 at a cyclic stress ratio of 0.41, as shown in Figure 21.

Several kinds of laboratory element tests have indicated that grouting CS can obviously improve the liquefaction resistance of loose sandy samples. CS gel forms in the gelation process and tends to bond sand particles together, which improve the strength of the soil structure and inhibits the generation of excess pore water pressure during the cyclic loading process. In the CS-treated ground improvement technique, CS concentration is a dominant factor that influences the strengthening effect. The higher the CS concentration is, the stronger the liquefaction resistance of the treated layers will be. In general, the investigated CS concentration in liquefaction mitigation varies from 5% to 20% in practical scenarios.

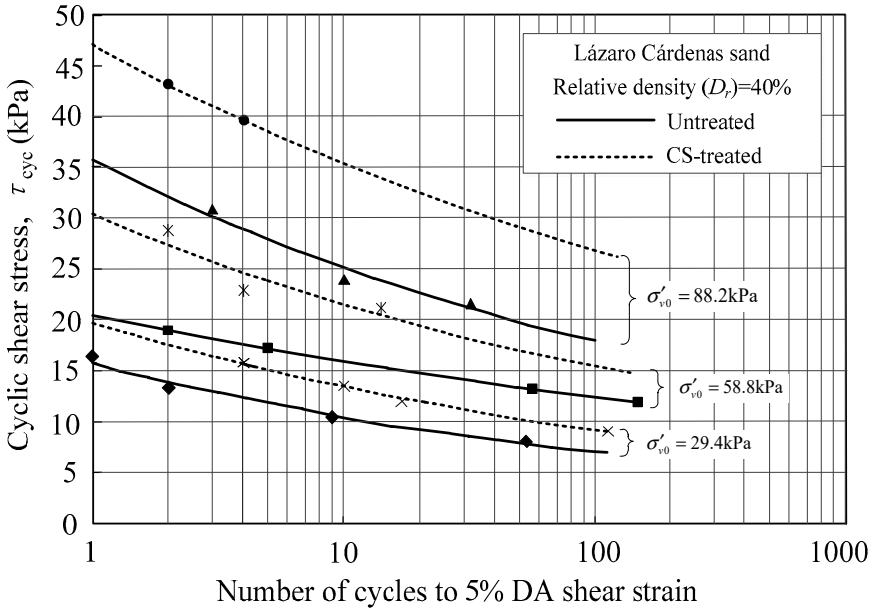

(**a**) Sample at 40% relative density

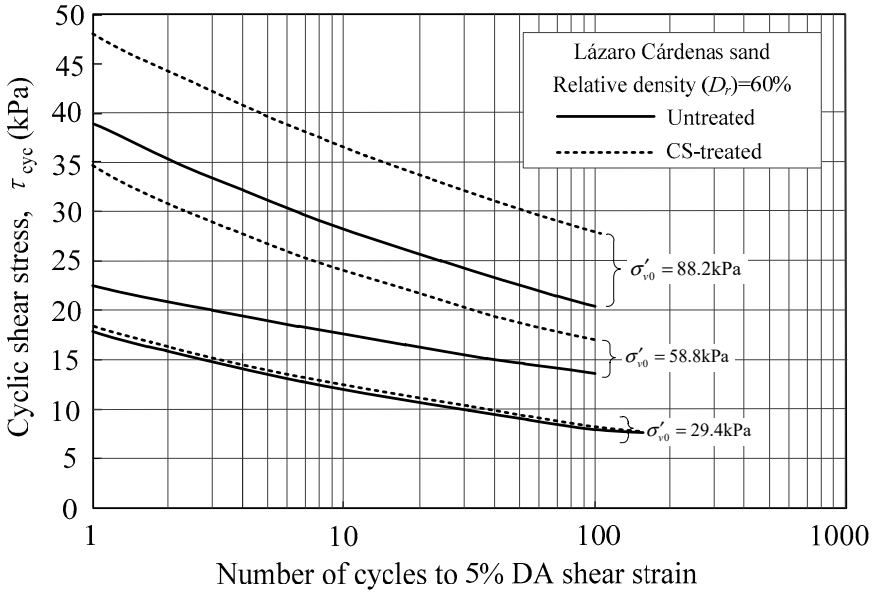

(**b**) Sample at 60% relative density

Figure 20. Comparison of cyclic resistance for untreated and CS-treated sand [17].

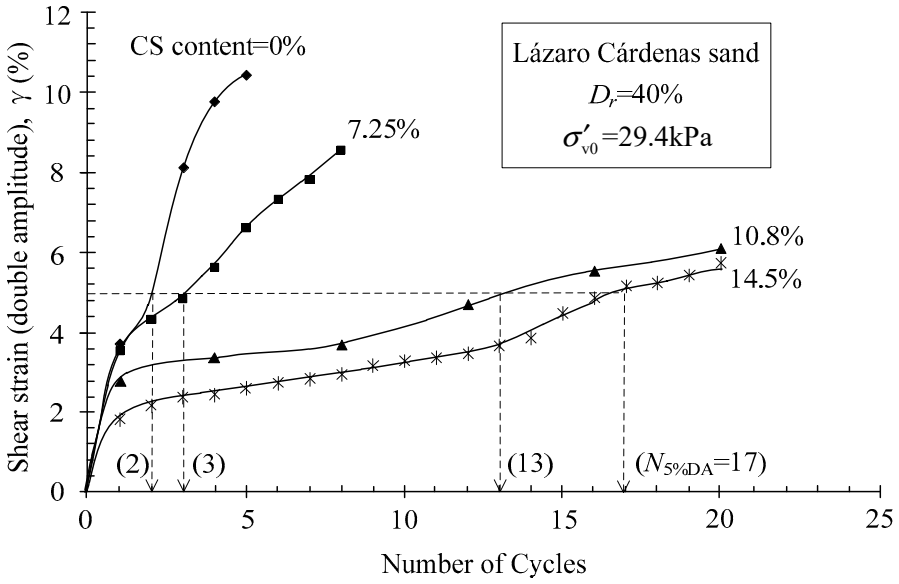

Figure 21. Shear strains for treated samples at various CS concentrations [17].

4.2. Centrifuge Model Behaviors of CS-Grouted Soil

Laboratory element experiments have indicated that CS-grouted soil has a sufficient ability to restrain DA strain and inhibit pore pressure generation, and, as such, it can mitigate liquefaction risk. However, the element test can only indicate the material properties of CS-soil mixtures. The structural behavior still needs to be investigated through model tests.

Taboada (1995) reported that significantly lower strains (~0.5–1%) were observed for the treated centrifuge models compared with the strains (~3–6%) of untreated model in the same kind of test [78]. Another centrifuge experiment was performed to verify the enhancing effect of CS grout to mitigate liquefaction risk for loose sand [7]. A laminar box composed of a stack of aluminum rings was used to provide a flexible-wall container. Grout supply ports were set at the bottom of the container to provide CS under a vacuum. The sand drain was pluviated around the grouting ports to permit the grouting material to permeate evenly into the sand, as shown in Figure 22. The CS was delivered through the soil with a saturation period of 13 h. Then, a firm, resonating gel formed after 56 h of gelling and a 240 h curing time. The prepared model was motivated by two shaking events, with 20 cycles of a 2 Hz sinusoidal input for each. The uniform peak accelerations were 0.2 g and 0.25 g, respectively. Lateral displacement and vertical settlement were measured by the linear variable differential transformers (LVDTs) mounted on the container rings at various depths. It was found that shear strains of 0.5% and 1% were observed during the first and second shake. Furthermore, only 30 mm settlement (0.3% strain) and 10 mm settlement (0.1% strain) were measured during the first and second episodes of shaking, respectively. The results demonstrate that the treated soil layer did not liquify during both shaking events, which provides evidence of the contribution of CS in mitigating liquefaction risk.

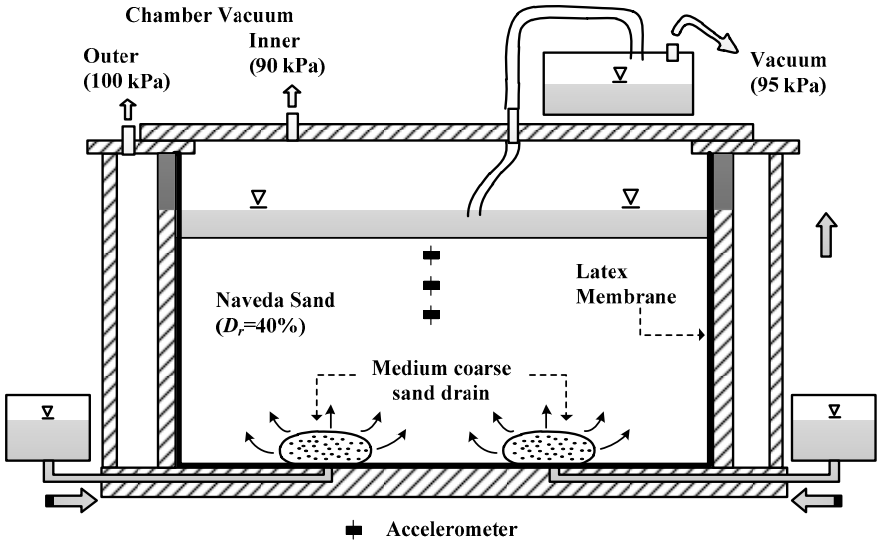

(**a**)

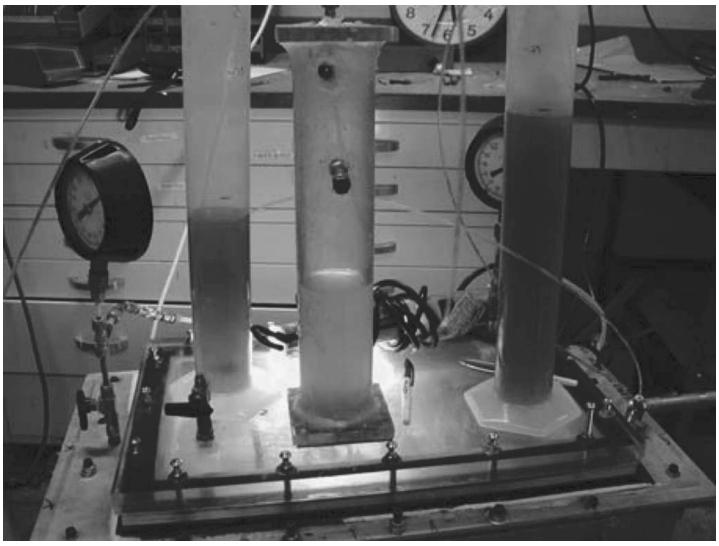

(**b**)

Figure 22. Model set for grouting: (**a**) Schematic for CS grouting in laminar box; (**b**) photograph of CS grouting [7].

Conlee et al. (2012) performed a well-designed centrifuge test to discuss the effect of CS concentration on the magnitude of cyclic shear strain for CS-treated models [40]. In the test, the container was mainly constructed with a 4.8 m-thick liquefiable loose sand layer and two slopes made up of loam that sloped 3° towards a 3 m-wide central channel. In test 1, one slope was grouted with 9% by weight CS (labelled CS-9), while the other was left untreated. In test 2, the two slopes were treated with 4% and 5% CS, labelled CS-4 and CS-5, respectively. Eight shaking events were applied to the model, with a centrifugal acceleration of 15 g. Immediately after test 1, large deformations occurred at the untreated side due to the liquefaction of the loose sand layer, and the upper loam slope was submerged in water. However, the treated side remain intact, as can be seen in Figure 23.

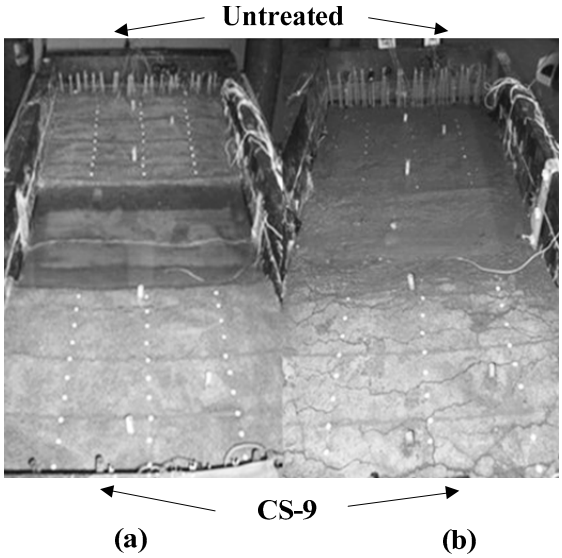

Figure 23. Model surface for test 1 (**a**) prior to the shaking events and (**b**) after the shaking events [40].

In addition, they also calculated the shear strains at different depths by double integration acceleration in time to obtain the transient displacement, and then differentiating in space. It was observed that the maximum shear strain γ_{max} in the untreated side reached up to 1% in shake 3, while γ_{max} was only 0.3% and 0.6% for CS-9 and CS-5, respectively. Similar reductions can be observed in shakes 4 and 5 (Figure 24). This experiment demonstrates that surface settlement and lateral spreading can be effectively controlled with CS treatment. CS grouting offers significant advantages for liquefiable sand layers overlain by existing structures that may be otherwise be difficult to treat by other methods. The results of the centrifuge model test are in agreement with those of the laboratory element test in demonstrating the mitigation effect of CS-grouted soil in terms of reducing liquefaction risk.

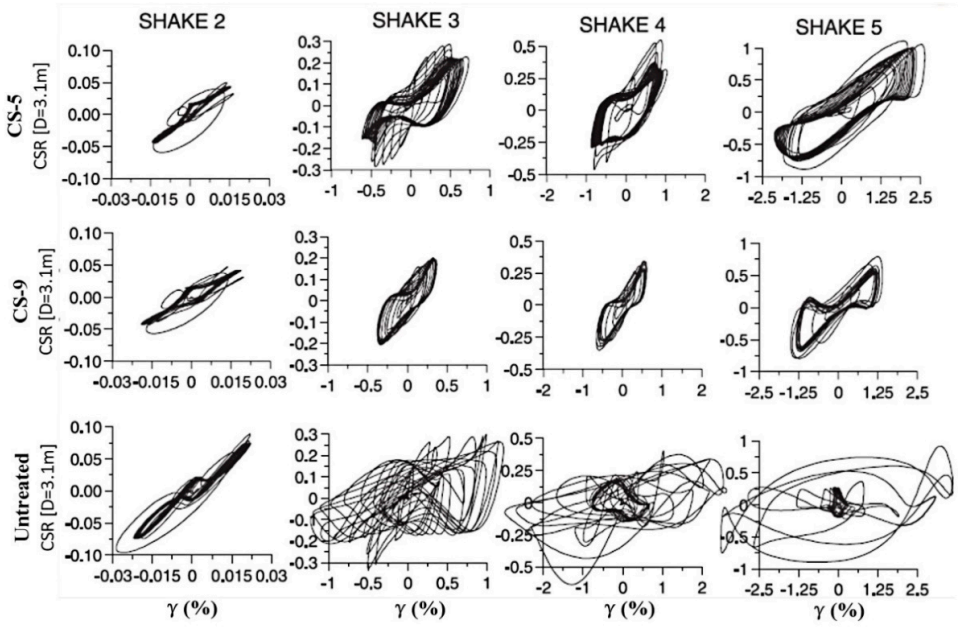

Figure 24. Cyclic stress ratio CSR against shear strain at the midpoint of liquefiable layer for the untreated, CS-9, and CS-5 samples [40].

4.3. Field Tests for Soils Grouted with CS

Since the performance of CS in soil improvement and liquefaction mitigation has been verified by a series of element and model tests, it was also justified by a field test conducted by Gallagher et al. (2007) [33]. The test site here was within a Canadian liquefaction experiment site located in Richmond, British Columbia. The soil stratigraphic sequence at the test site is characterized by a sand and silty sand layer at the surface, overlain over a layer of silt and sandy silt, following a 10 m liquefiable layer of sand to silty sand, buried at a depth of 5–15 m [79]. At the treated area, eight injection wells were spaced equally around the perimeter of a 9 m-diameter circle, with an extraction well at the center. Two injection stages were used for the injection well to permeate CS into the soil layers buried at depths of 6.5–7.5 m and 7.5–8.5 m, respectively. An injection well is designed to inject more than 7000 L of CS at a concentration of 7%. As a matter of fact, since some malfunctions occurred during the injection process, only 45,000 L of diluted CS suspensions were finally injected in the field test. After the grouting injection was completed, two decks of Pentolite 50/50 explosives were installed at each injection well to create blast-induced liquefaction. At the untreated area adjacent to the treated one, eight similar wells were excavated as blast holes to accommodate explosives, as shown in Figure 25. Six survey lines extended from the center, and a total of 14 settlement measurements were taken along each ray.

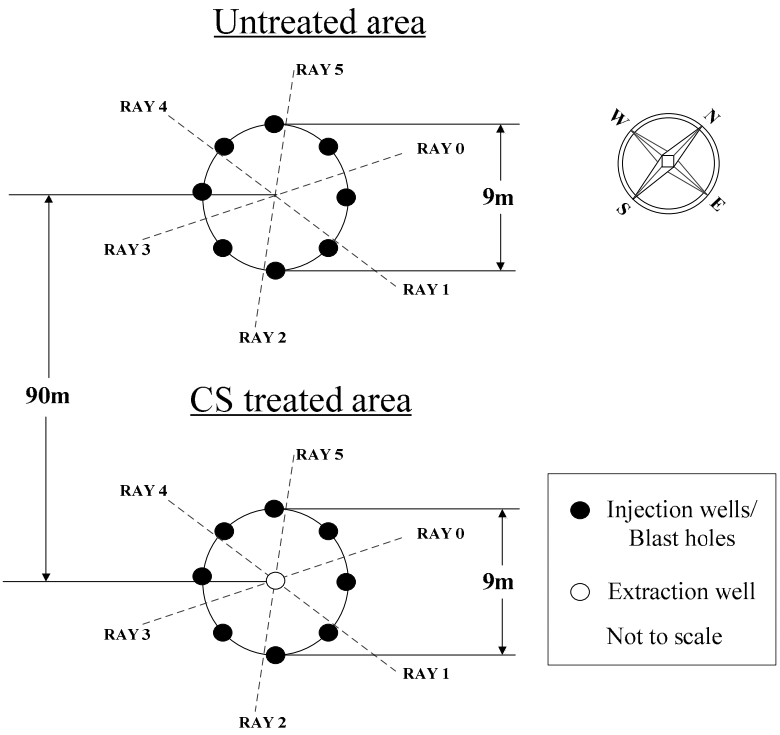

Figure 25. Site layout for full-scale test (modified after Gallagher et al., 2007) [33].

Excess pore pressure was monitored in the treated area. The excess pore pressure ratio R_u was adopted to indicate the evolutive law of pore water pressure. It was shown that R_u reached 1, even in the treated area, indicating the grouted layer can be considered to have liquified here. However, the settlement measurements indicate that a maximum settlement of 0.5 m was recorded in the untreated area, while the maximum settlement reduced to 0.3 m in the treated area (Figure 26). Moreover, Gallagher et al. (2007) deduced that the 0.3 m deformation mainly occurred in the untreated layer, and the reduction in settlement should be attributed to the grouted layer (at depths of 6.5–8.5 m). They believed that the majority of settlement would be prevented if the entire layer was grouted.

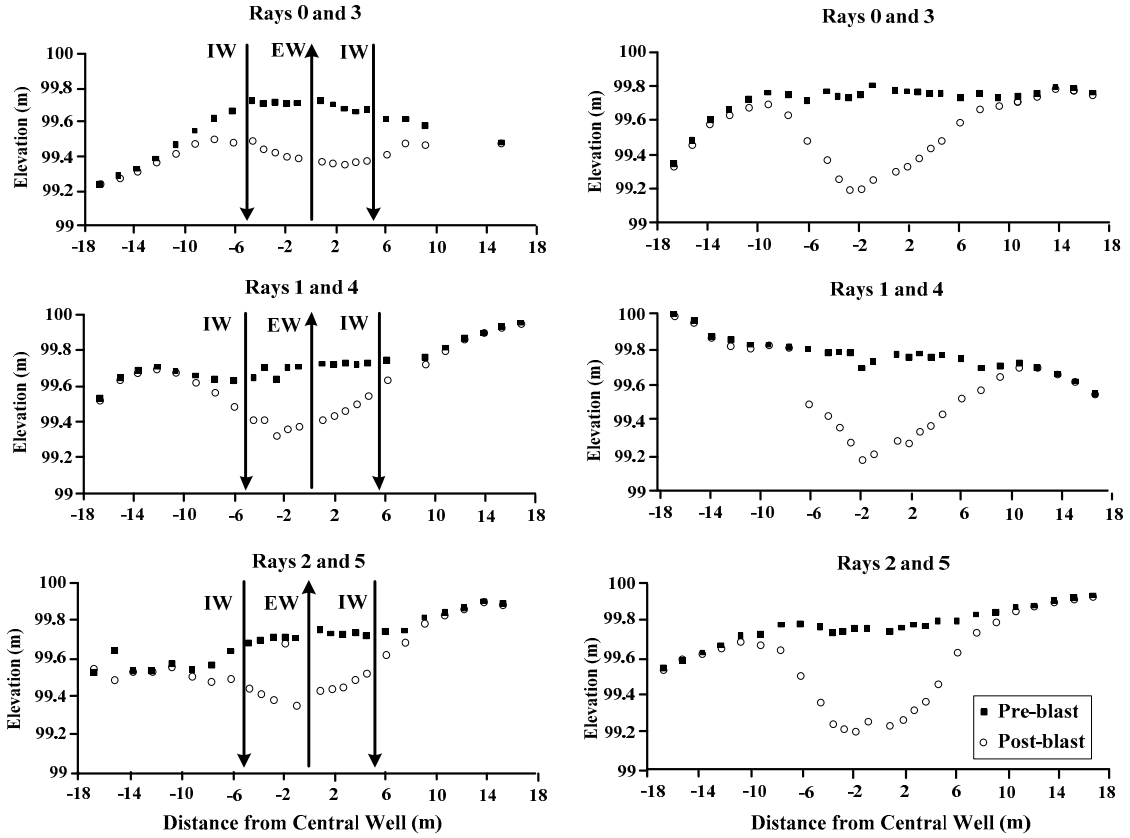

Figure 26. Elevation profile prior to and after blasting in full-scale test [33].

Conlee (2010) then performed another field test to investigate the mitigation effect of CS grouting on liquefaction damage [66]. In this field experiment, CS was grouted and transported to treat a 1.5 m-thick, poorly graded sand layer, with an area of 9.3 m^2. In the preliminary test layout, two kinds of grouting techniques, including mandrel injection and the well/packer injection method, were planned to be adopted to permeate CS to the targeted area. Furthermore, a TRex mobile shaker was intended to be used to induce liquefaction, and the targeted area was set hexagonally to match the shaker pad of the TRex shaker [66,80]. However, two dominant difficulties were presented in the field. First of all, the mandrel injection method proved to be unsuccessful in practice. Secondly, the measured pore pressure response indicated no significant increases in pore water pressure in vibro-seismic shaking when using TRex shaker. Thus, it is uncertain whether the TRex shaker will produce remarkable shear strains and initiate liquefaction at greater depths. Therefore, the packer injection method was finally adopted, and mandrel replaced TRex mobile shaker to induce liquefaction. The mandrel was equipped with a vibratory hammer to supply the excitation. For each ground motion, the vibratory hammer was employed as the steel mandrel and was driven into the ground to a maximum depth of 6 m. As the mandrel is driven to produce a combination of compression waves and shear waves, complex shearing in deeper soil deposits is initiated, and liquefaction can be achieved in larger depths.

Shear strain was measured by liquefaction sensors in both the horizontal (X-Y) and vertical (Y-Z and X-Z) planes. Each liquefaction sensor consisted of 3 accelerometers that formed a triangular array. For each accelerometer, motions were recorded in the X, Y, and Z axes. In this way, shear strains were obtained in X-Y, Y-Z, and X-Z directions. The shear strains, which predominantly occurred in the X-Y and Y-Z axes in the untreated area, reached 0.05% in both directions. Even the shear strain in the X-Z direction increased beyond 0.01% in the original area. However, after being grouted with CS, the shear strains measured in the treated area reduced significantly in all three of these directions. Except for the shear strain in the X-Y direction at 12 s, which arrived at 0.025%, the others remained below 0.01% throughout the whole experiment process. The results indicate that permeation of CS

gel will aid in decreasing the shear strain occurred during cyclic loading and improving liquefaction resistance for liquefiable ground.

The experimental element tests, centrifuge tests, and field tests performed in the literature have shown that CS has potential application in improving ground conditions and mitigating liquefaction in an earthquake event. By grouting CS, both the settlement and shear strain during the cyclic loading process decrease, and the generation of pore water pressure is inhibited. However, some problems still exist in the grouting process. The field test conducted by Gallagher et al. (2007) [33], for example, suffered some grouting failures in three injection holes. These failures lead to a significant reduction in the injected CS volume compared to the other holes. Post-treatment analysis showed that the failure could be attributed to the gelation of CS grouted in other boreholes and the return of grout around the annulus. Nevertheless, the treated area still produced less settlement in a blast-induced liquefaction, indicating the remarkable effect of CS in mitigating liquefaction.

5. Prospect of Colloidal Silica as a Grouting Material

5.1. Other Applications for CS in Civil Engineering

CS is a kind of promising nanomaterial and has various potential applications in other branches of civil engineering. Apart from ground improvement and liquefaction mitigation, CS has been investigated by some researchers to be used for controlling water production and fluid flow in the petroleum industry, reducing permeability and fixing contaminants in environmental engineering, and preventing water ingress in underground and tunneling construction.

Jurinak and Summers (1991) used CS in a practical reservoir fluid-flow control system for workovers at an oilfield [81]. Eleven wells were treated with CS for water injection profile modification, water production control, and remedial casing repair. The results show that CS treatment works well in water production control and remedial casing repair. Zones that have been previously hydraulically fractured can be perfectly treated using CS. Moreover, CS has also been verified to be suitable as a permeation grout for barrier systems in contaminated sites [82–85]. Moridis et al. (1995) used CS when injecting in a heterogeneous unsaturated sand layer at 10–14 feet in depth. It was shown that CS could effectively permeate through this porous media and form a fairly uniform plume. A post-treatment test showed a four order of magnitude permeability reduction for the treated layers. Thus, CS is a potential material that can remarkably decrease hydraulic conductivity and, therefore, can be adopted for use in contaminant barrier systems [82]. Manchester et al. (2001) injected CS gel into large sand tanks to determine in situ hydraulic conductivity. Consequently, a permeation test indicated that by grouting CS, a core approximately 60 cm in diameter was produced, with a remarkable reduction in saturated hydraulic conductivity [85]. Besides, the soil-water characteristic curves of grouted soils further verified the use of CS as a grouting material to isolate activated soils in the vadose zone.

In addition, CS can also be adopted as grouting agent to permeate through hard rocks in tunneling and underground engineering. Geotechnical procedures were adopted to analyze silica soil's mechanical behaviors over time and in different storage conditions, representing different environments encountered in tunnels [86,87]. It was shown that the initial strength of silica soil increases faster at high temperatures or low humidity, indicating sufficient strength can be obtained in this instance to withstand most grouting conditions. Moreover, when sufficiently confined, silica soil is ductile. These properties indicate that it can suffer loading and unloading cycles in fairly large deformations. Meanwhile, a hydraulic conductivity between 10^{-10} and 10^{-11} m/s was observed for silica soil, which implies that silica soil is a kind of low permeation material and is a suitable material to be grouted in hard rocks in tunneling practice.

5.2. Advantages of CS as a Grouting Material

5.2.1. Low Disturbance

Among ground improvement techniques, dynamic compaction, vibro-compaction and explosive compaction have been widely adopted to densify soil layers. However, all of these compaction methods produce great disturbances to the surrounding areas and are not applicable to solely the constrained or developed area. Except for the compaction methods, the grouting method is another common practice to improve ground liquefaction resistance. In all grouting materials, a cement-based material is mostly used. Nevertheless, the particle size of cement averages at 20 microns, which greatly restricts its permeation properties. Cement particles can only transport through voids three to five times larger than their own particle size [15]. Besides, cement has a relatively high initial viscosity, so cement is usually injected under pressure or is adopted to form grout columns, rather than distribution through the entire ground. In addition, grouting cement has a remarkable impact to the surrounding environment. Since conventional methods show great disturbance, grouting CS is an effective method and presents significant advantages over cement. CS has a very low initial viscosity which is very close to pure water once mixed with an electrolyte. The low initial viscosity provides excellent flowability to the grouting materials. Additionally, the particle size of CS ranges from 7–20 nm in general, which is much finer than cement particles. Thus, CS can achieve transport through the entire targeted scope in the porous media under a low pressure. Therefore, grouting CS for ground improvement is feasible for both undeveloped and constrained areas, as it only has low levels of disturbance to the surrounding area.

5.2.2. Environmentally Friendly

The production of cement is an energy-intensive process which consumes massive amounts of coal, discharging many harmful gases in the production process [88]. The chemical grouting materials, such as acrylamide, polyurethane, and epoxy, have better penetrability when compared to cement-based grouting materials, but they are expensive and may cause pollution to underground waterways if handled improperly [89]. The poisoning incident of Fukuoka in 1974, for example, was caused by acrylamide grouting materials for ground improvement. Since then, Japan's Ministry of Construction has set rules that allow only soluble silica to be adopted as a chemical grouting material to improve liquefaction resistance [90]. CS is a kind of nanomaterial and a derivative of soluble silica. It is nontoxic, chemically and biologically inert, and environmentally friendly. When added to soil as a grouting material, CS will not cause pollution, which is known on a basis of learned knowledge. Environmental scientists have also noted that great attention should be paid to the behaviors and application of nanomaterials, with CS included. Thus, CS is a practically potential grouting material due to its environmental-friendly feature.

5.2.3. Low Cost

The price/performance ratios of CS and some other chemical solutions have been analyzed in detail. [15,44]. Although the unit price of CS is relatively high, only a spot of CS is effective for liquefaction mitigation. Each cubic meter of treated soil consumes CS that costs 59 USD when CS concentration is controlled to be 5% [15]. However, the treatment costs are about 180, 325, and 500 USD per cubic meter of grouted soil for sodium silica, acrylamide, and epoxy respectively. Thus, CS is such an economical material that its treatment cost is less than one third of the cost of the traditional chemical solutions.

Meanwhile, with the booming advancement of nanotechnology practices worldwide, the price of nanomaterials is expected to largely decrease [91]. For instance, the price of carbon nanotubes has significantly fallen from 150 USD per gram in 2000 to 50 USD per gram in 2010. Thus, it can be deduced that CS, as a kind of nanomaterial, will become much cheaper than its current price in the future. As noted by Huang and Wang (2016), although the application of CS for ground improvement and

liquefaction mitigation is still in experimental study stage, it will finally be successful for commercial use, due to the advantages of CS in terms of both the environmental and cost aspects [15].

6. Conclusions

With the astonishing development of nanotechnology, nanomaterials are beginning to extensively be adopted in civil engineering, due to their apparent advantages of being cost-effective, with low disturbance, and being environmentally friendly. Colloidal silica (CS), which has been shown to have the ability of mitigating liquefaction, is a kind of such nanomaterial with high cost performance. This paper has reviewed this innovative technique by using CS for ground improvement and liquefaction mitigation. Specially, the critical factors that can significantly influence CS transport and the CS strengthening effect were discussed in detail. Based on the conclusions drawn from the previous literature, it was summarized in this paper that the CS concentration and curing time are the two dominant factors that determine the ground improvement effect. Moreover, the fact that CS can greatly mitigate liquefaction for loose sand layers is widely recognized. However, this CS-based soil liquefaction mitigation technique still faces certain challenges associated with control of the gelling time, the CS injection success rate, CS delivery with minimum deposition, and so on. It is of great concern to further develop the approaches to transport CS to the targeted location as precisely as possible with minimum deposition. To settle this issue, ongoing studies should focus on both the gelation properties and the permeation ability of CS in porous media. Although a CS-based soil stabilization technique was put forward after 2000 and is still in the preliminary study and application process, we are pleased to find that this innovative technique was adopted to treat the runways at Fukuoka International Airport in 2016. It is promising that by settling the current challenges, the CS-based liquefaction mitigation technique will ripen gradually and can be expected to be widely adopted in future anti-seismic projects.

Author Contributions: Conceptualization, G.L. and M.Z.; methodology, M.Z. and G.L.; formal analysis, M.Z. and C.Z.; investigation, M.Z., W.G. and C.Z.; writing-original manuscript preparation, M.Z. and G.L.; writing-review and editing, M.Z., G.L., W.G. and Q.L. All authors have read and agreed to the published version of the manuscript.

Funding: This research was funded by National Science Foundation of China, grant number 51408491 and 51878560.

Conflicts of Interest: The authors declare no conflict of interest.

References

1. Reddy, A.S.; Srinivasan, R. Analysis of Soil Liquefaction: Niigata Earthquake. *J. Soil Mech. Found. Div.* **1967**, *93*, 83–108.
2. Ross, G.A.; Seed, H.B.; Migliaccio, R.R. Bridge Foundation Behavior in Alaska Earthquake. *J. Soil Mech. Found. Div.* **1969**, *95*, 1007–1036.
3. Singh, S.K.; Suarez, G. *Review of the Seismicity of Mexico with Emphasis on the September 1985*; Michoacan Earthquakes, Instituto de Geofísica, UNAM: Mexico City, Mexico, 1986.
4. Elgamal, A.W.; Zeghal, M.; Parra, E. Liquefaction of reclaimed island in Kobe, Japan. *J. Geotech. Eng.* **1996**, *122*, 39–49. [CrossRef]
5. Juang, C.H.; Li, D.K. Assessment of liquefaction hazards in Charleston quadrangle, South Carolina. *Eng. Geol.* **2007**, *92*, 59–72. [CrossRef]
6. Huang, Y.; Yu, M. Review of soil liquefaction characteristics during major earthquakes of the twenty-first century. *Nat. Hazards* **2013**, *65*, 2375–2384. [CrossRef]
7. Gallagher, P.M.; Pamuk, A.; Abdoun, T. Stabilization of Liquefiable Soils Using Colloidal Silica Grout. *J. Mater. Civ. Eng.* **2007**, *19*, 33–40. [CrossRef]
8. Ishihara, K.; Yasuda, S.; Nagase, H. Soil characteristics and ground damage. *Soils Found.* **1996**, *36*, 109–118. [CrossRef]
9. Dobry, R.; Abdoun, T. Post-Triggering Response of Liquefied Sand in the Free Field and Near Foundations. *Geotech. Spec. Publ.* **1998**, *75*, 270–300.

10. Dappolonia, E.; Miller, C.E.; Ware, T.M. Sand Compaction by Vibroflotation. *Trans. Am. Soc. Civil Eng.* **1955**, *120*, 154–168.
11. Menard, L.; Broise, Y. Theoretical and practical aspect of dynamic consolidation. *Geotechnique* **1975**, *25*, 3–18. [CrossRef]
12. Mayne, P.W.; Jones, J.S.; Dumas, J.C. Ground Response to Dynamic Compaction. *J. Geotech. Eng.* **1984**, *110*, 757–774. [CrossRef]
13. Welsh, J.P. In situ testing for ground modification techniques. In *Use of In Situ Tests in Geotechnical Engineering*; ASCE: Reston, VA, USA, 1986; pp. 322–335.
14. Mollamahmutoglu, M.; Yilmaz, Y. Pre-and post-cyclic loading strength of silica-grouted sand. *Proc. Inst. Civ. Eng. Geotech. Eng.* **2010**, *163*, 343–348. [CrossRef]
15. Huang, Y.; Wang, L. Experimental studies on nanomaterials for soil improvement: A review. *Environ. Earth Sci.* **2016**, *75*, 497. [CrossRef]
16. Tsuchida, H. Prediction and remedial measures against liquefaction of sandy soil. In *Annual Seminar of Port and Harbour Research Institute*; International Association of Ports and Harbors: Tokyo, Japan, 1970; Volume 3, pp. 1–33.
17. Díaz-Rodríguez, J.A.; Antonio-Izarraras, V.M.; Bandini, P.; López-Molina, J.A. Cyclic strength of a natural liquefiable sand stabilized with colloidal silica grout. *Can. Geotech. J.* **2008**, *45*, 1345–1355. [CrossRef]
18. Yonekura, R.; Miwa, M. Fundamental properties of sodium silicate based grout. In Proceedings of the 11th Southeast Asia Geotechnical Conference, Singapore, 4–8 May 1993; Volume 439.
19. Persoff, P.; Apps, J.; Moridis, G.; Whang, J.M. Effect of dilution and contaminants on sand grouted with colloidal silica. *J. Geotech. Geoenviron. Eng.* **1999**, *125*, 461–469. [CrossRef]
20. Kodaka, T.; Ohno, Y.; Takyu, T. Cyclic shear characteristics of treated sand with colloidal silica grout. In Proceedings of the International Conference on Soil Mechanics and Geotechnical Engineering, Osaka, Japan, 12–16 September 2005; Aa Balkema Publishers: Amstelredam, The Netherlands, 2005; Volume 16, p. 401.
21. Tong, Z.; Bischoff, M.; Nies, L.; Applegate, B.; Turco, R.F. Impact of fullerene (C60) on a soil microbial community. *Environ. Sci. Technol.* **2007**, *41*, 2985–2991. [CrossRef] [PubMed]
22. Johansen, A.; Pedersen, A.L.; Jensen, K.A.; Karlson, U.; Hansen, B.M.; Scott-Fordsmand, J.J.; Winding, A. Effects of C60 fullerene nanoparticles on soil bacteria and protozoans. *Environ. Toxicol. Chem. Int. J.* **2008**, *27*, 1895–1903. [CrossRef]
23. El Mohtar, C.S.; Bobet, A.; Santagata, M.C.; Drnevich, V.P.; Johnston, C.T. Liquefaction mitigation using bentonite suspensions. *J. Geotech. Geoenviron. Eng.* **2012**, *139*, 1369–1380. [CrossRef]
24. Arabania, M.; Haghib, A.K.; Moradic, Y. Evaluation of mechanical properties improvement of clayey sand by using carbon nanotubes. In Proceedings of the 4th International Conference on Nanostructures (ICNS4), Kish Island, Iran, 12–14 March 2012; pp. 1567–1569.
25. Huang, Y.; Wang, L. Laboratory investigation of liquefaction mitigation in silty sand using nanoparticles. *Eng. Geol.* **2016**, *204*, 23–32. [CrossRef]
26. Feynman, R.P. There's plenty of room at the bottom. *Calif. Inst. Technol. Eng. Sci. Mag.* **1960**, *23*, 22–36.
27. Luo, H.L.; Hsiao, D.H.; Lin, D.F.; Lin, C.K. Cohesive soil stabilized using sewage sludge ash/cement and nano aluminum oxide. *Int. J. Transp. Sci. Technol.* **2012**, *1*, 83–99. [CrossRef]
28. Niroumand, H.; Zain, M.F.M.; Alhosseini, S.N. The influence of nano-clays on compressive strength of earth bricks as sustainable materials. *Procedia Soc. Behav. Sci.* **2013**, *89*, 862–865. [CrossRef]
29. Taha, M.R.; Taha, O.M. Crack control of landfill liner and cap materials using nano-alumina powder. *Coupled Phenom. Environ. Geotech.* **2013**, *215*, 459–463.
30. Zhang, G.; Germaine, J.T.; Whittle, A.J.; Ladd, C.C. Index properties of a highly weathered old alluvium. *Geotechnique* **2004**, *54*, 441–451. [CrossRef]
31. Bahmani, S.H.; Huat, B.B.; Asadi, A.; Farzadnia, N. Stabilization of residual soil using SiO2 nanoparticles and cement. *Constr. Build. Mater.* **2014**, *64*, 350–359. [CrossRef]
32. Gallagher, P.M.; Mitchell, J.K. Influence of colloidal silica grout on liquefaction potential and cyclic undrained behavior of loose sand. *Soil Dyn. Earthq. Eng.* **2002**, *22*, 1017–1026. [CrossRef]
33. Gallagher, P.M.; Conlee, C.T.; Rollins, K.M. Full-scale field testing of colloidal silica grouting for mitigation of liquefaction risk. *J. Geotech. Geoenviron. Eng.* **2007**, *133*, 186–196. [CrossRef]
34. Liao, H.J.; Huang, C.C.; Chao, B.S. Liquefaction resistance of a colloid silica grouted sand. In *Grouting and Ground Treatment*; ASCE: Reston, VA, USA, 2003; pp. 1305–1313.

35. Kakavand, A.; Dabiri, R. Experimental study of applying colloidal nano Silica in improving sand-silt mixtures. *Int. J. Nano Dimens.* **2018**, *9*, 357–373.
36. Agapoulaki, G.I.; Papadimitriou, A.G. Rheological Properties of Colloidal Silica Grout for Passive Stabilization Against Liquefaction. *J. Mater. Civ. Eng.* **2018**, *30*, 04018251. [CrossRef]
37. Rasouli, R.; Hayashi, K.; Zen, K. Controlled permeation grouting method for mitigation of liquefaction. *J. Geotech. Geoenviron. Eng.* **2016**, *142*, 04016052. [CrossRef]
38. Iler, R.K. *The Chemistry of Silica: Solubility, Polymerization, Colloid and Surface Properties*; Wiley: New York, NY, USA, 1979.
39. Whang, J.M. Section 9—Chemical-based barrier materials. In *Assessment of Barrier Containment Technologies for Environmental Remediation Applications*; Rumer, R.R., Mitchell, J.K., Eds.; NTIS: Springfield, VA, USA, 1995; pp. 211–247.
40. Conlee, C.T.; Gallagher, P.M.; Boulanger, R.W.; Kamai, R. Centrifuge modeling for liquefaction mitigation using colloidal silica stabilizer. *J. Geotech. Geoenviron. Eng.* **2012**, *138*, 1334–1345. [CrossRef]
41. DuPont. *Ludox Colloidal Silica: Properties, Uses, Storage, and Handling, Production Information*; DuPont: Wilmington, NC, USA, 1997.
42. Gallagher, P.M. Passive Site Remediation for Mitigation of Liquefaction Risk. Ph.D. Thesis, Virginia Tech, Blacksburg, VA, USA, 2000.
43. Spencer, L.; Rix, G.J.; Gallagher, P. Colloidal silica gel and sand mixture dynamic properties. In *Geotechnical Earthquake Engineering and Soil Dynamics IV*; ASCE: Reston, VA, USA, 2008; pp. 1–10.
44. Bao, X.; Jin, Z.; Cui, H.; Chen, X.; Xie, X. Soil liquefaction mitigation in geotechnical engineering: An overview of recently developed methods. *Soil Dyn. Earthq. Eng.* **2019**, *120*, 273–291. [CrossRef]
45. Gallagher, P.M.; Lin, Y. Colloidal silica transport through liquefiable porous media. *J. Geotech. Geoenviron. Eng.* **2009**, *135*, 1702–1712. [CrossRef]
46. Otterstedt, J.-E.; Greenwood, P. Some important, fairly new uses of colloidal silica/silica soil. In *Fundamentals and Applications*; Chapter 57 in Colloidal silica; Bergna, H., Roberts, W.O., Eds.; Taylor & Francis: Abingdon upon Thames, UK, 2005.
47. Koch, A.J. Model Testing of Passive Site Stabilization. Ph.D. Thesis, Drexel University, Philadelphia, PA, USA, 2002.
48. Lin, Y. Colloidal Silica Transport Mechanisms for Passive Site Stabilization of Liquefiable Soils. Ph.D. Thesis, Drexel University, Philadelphia, PA, USA, 2006.
49. Persoff, P.; Moridis, G.J.; Apps, J.A.; Pruess, K. Evaluation tests for colloidal silica for use in grouting applications. *Geotech. Test. J.* **1998**, *21*, 264–269.
50. Wong, C.; Pedrotti, M.; El Mountassir, G.; Lunn, R.J. A study on the mechanical interaction between soil and colloidal silica gel for ground improvement. *Eng. Geol.* **2018**, *243*, 84–100. [CrossRef]
51. Pedrotti, M.; Wong, C.; El Mountassir, G.; Lunn, R.J. An analytical model for the control of silica grout penetration in natural groundwater systems. *Tunn. Undergr. Space Technol.* **2017**, *70*, 105–113. [CrossRef]
52. Aldaood, A.; Bouasker, M.; Al-Mukhtar, M. Impact of freeze–thaw cycles on mechanical behaviour of lime stabilized gypseous soils. *Cold Reg. Sci. Technol.* **2014**, *99*, 38–45. [CrossRef]
53. Hotineanu, A.; Bouasker, M.; Aldaood, A.; Al-Mukhtar, M. Effect of freeze–thaw cycling on the mechanical properties of lime-stabilized expansive clays. *Cold Reg. Sci. Technol.* **2015**, *119*, 151–157. [CrossRef]
54. Seyedi, S.; Mirkazemi, S.; Baziar, M. Application of nanomaterial to stabilize a weak soil. In Proceedings of the Seventh International Conference on Case Histories in Geotechnical Engineering, Chicago, IL, USA, 29 April–4 May 2013.
55. Majeed, Z.H.; Taha, M.R. Effect of nanomaterial treatment on geotechnical properties of a Penang soft soil. *J. Asian Sci. Res.* **2012**, *2*, 587.
56. Ghasabkolaei, N.; Choobbasti, A.J.; Roshan, N.; Ghasemi, S.E. Geotechnical properties of the soils modified with nanomaterials: A comprehensive review. *Arch. Civil Mech. Eng.* **2017**, *17*, 639–650. [CrossRef]
57. Noll, M.R.; Bartlett, C.; Dochat, T.M. In situ permeability reduction and chemical fixation using colloidal silica. In Proceedings of the Sixth National Outdoor Action Conference on Aquifer Restoration, Ground Water Monitoring, and Geophysical Method, State College, PA, USA, 11–13 May 1992; National Ground Water Association: Westerville, OH, USA, 1992.
58. Changizi, F.; Haddad, A. Strength properties of soft clay treated with mixture of nano-SiO2 and recycled polyester fiber. *J. Rock Mech. Geotech. Eng.* **2015**, *7*, 367–378. [CrossRef]

59. Ryan, J.N.; Elimelech, M.; Ard, R.A.; Harvey, R.W.; Johnson, P.R. Bacteriophage PRD1 and silica colloid transport and recovery in an iron oxide-coated sand aquifer. *Environ. Sci. Technol.* **1999**, *33*, 63–73. [CrossRef]
60. Higgo, J.J.W.; Williams, G.M.; Harrison, I.; Warwick, P.; Gardiner, M.P.; Longworth, G. Colloid transport in a glacial sand aquifer. Laboratory and field studies. In *Colloids in the Aquatic Environment*; Elsevier: Amsterdam, The Netherlands, 1993; pp. 179–200.
61. Saiers, J.E.; Hornberger, G.M.; Harvey, C. Colloidal silica transport through structured, heterogeneous porous media. *J. Hydrol.* **1994**, *163*, 271–288. [CrossRef]
62. Ryan, J.N.; Elimelech, M. Colloid mobilization and transport in groundwater. *Colloids Surf. A Physicochem. Eng. Asp.* **1996**, *107*, 1–56. [CrossRef]
63. Johnson, P.R.; Sun, N.; Elimelech, M. Colloid transport in geochemically heterogeneous porous media: Modeling and measurements. *Environ. Sci. Technol.* **1996**, *30*, 3284–3293. [CrossRef]
64. Gallagher, P.M.; Koch, A.J. Model testing of passive site stabilization: A new grouting technique. In *Grouting and Ground Treatment*; American Society of Civil Engineers: Preston, VA, USA, 2003; pp. 1478–1489.
65. Gallagher, P.M.; Finsterle, S. Physical and numerical model of colloidal silica injection for passive site stabilization. *Vadose Zone J.* **2004**, *3*, 917–925. [CrossRef]
66. Conlee, C.T. Dynamic Properties of Colloidal Silica Soils Using Centrifuge Model Tests and a Full-Scale Field Test. Ph.D. Thesis, Drexel University, Philadelphia, PA, USA, 2010.
67. Hamderi, M.; Gallagher, P.M. An optimization study on the delivery distance of colloidal silica. *Sci. Res. Essays* **2013**, *8*, 1314–1323.
68. Hamderi, M.; Gallagher, P.M.; Lin, Y. Numerical model for colloidal silica injected column tests. *Vadose Zone J.* **2014**, *13*, vzj2013.07.0138. [CrossRef]
69. Hamderi, M.; Gallagher, P.M. Pilot-scale modeling of colloidal silica delivery to liquefiable sands. *Soils Found.* **2015**, *55*, 143–153. [CrossRef]
70. Zen, K.; Hayashi, K.; Yamazaki, H.; Hirasawa, M. Variations of liquefaction strength induced by the different injection processes in the permeation grouting method. In Proceedings of the XV Danube-European Conference on Geotechnical Engineering, Vienna, Austria, 9–11 September 2014.
71. Burton, M.B. Method and Apparatus for Lateral Drilling in Oil and Gas Wells. U.S. Patent No. 4699224, 13 October 1987.
72. Karlsson, H.; Jacques, G.E.; Hatten, J.L.; Aslakson, J.K. Method and Apparatus for Horizontal Drilling. U.S. Patent No. 5148875, 22 September 1992.
73. Clough, G.W.; Iwabuchi, J.; Rad, N.S.; Kuppusamy, T. Influence of cementation on liquefaction of sands. *J. Geotech. Eng.* **1989**, *115*, 1102–1117. [CrossRef]
74. Towhata, I.; Kabashima, Y. Mitigation of seismically-induced deformation of loose sandy foundation by uniform permeation grouting. In Proceedings of the Earthquake Geotechnical Engineering Satellite Conference, XVth International Conference on Soil Mechanics and Geotechnical Engineering, Istanbul, Turkey, 27–31 August 2001; pp. 313–318.
75. Seed, H.B. *Ground Motions and Soil Liquefaction during Earthquakes*; Earthquake Engineering Research Insititue: Oakland, CA, USA, 1982.
76. Díaz-Rodríguez, J.A.; Antonio-Izarraras, V.M. Mitigation of liquefaction risk using colloidal silica. In Proceedings of the 13th World Conference on Earthquake Engineering, Vancouver, BC, Canada, 1–6 August 2004; pp. 1–6.
77. Kodaka, T.; Oka, F.; Ohno, Y.; Takyu, T.; Yamasaki, N. Modeling of cyclic deformation and strength characteristics of silica treated sand. In *Geomechanics: Testing, Modeling, and Simulation*; ASCE: Reston, VA, USA, 2005; pp. 205–216.
78. Taboada, V.M. Centrifuge Modeling of Earthquake-Induced Lateral Spreading in Sand Using a Laminar Box. Ph.D. Thesis, Rensselaer Polytechnic Institute, Troy, NY, USA, 1995.
79. Rollins, K.M.; Anderson, J.K.; McCain, A.K.; Goughnour, R.R. Vertical composite drains for mitigating liquefaction hazard. In Proceedings of the Thirteenth International Offshore and Polar Engineering Conference, Honolulu, HI, USA, 25–30 May 2003; International Society of Offshore and Polar Engineers: Mountain View, CA, USA, 2003.
80. Nenad, G. Using Large Mobile Shakers for Non-Destructive Infrastructure Testing. Available online: https://www.designsafe-ci.org/community/news/2018/november/using-large-mobile-shakers-non-destructive-infrastructure-tests/ (accessed on 4 November 2019).

81. Jurinak, J.J.; Summers, L.E. Oilfield applications of colloidal silica gel. *Spe Prod. Eng.* **1991**, *6*, 406–412. [CrossRef]
82. Moridis, G.J.; Persoff, P.; Apps, J.A.; Myer, L.; Pruess, K.; Yen, P. *A Field Test of Permeation Grouting in Heterogeneous Soils Using a New Generation of Barrier Liquids*; Lawrence Berkeley Lab.: Berkeley, CA, USA, 1995.
83. Moridis, G.; Apps, J.; Persoff, P.; Myer, L.; Muller, S.; Pruess, K.; Yen, P. *A Field Test of a Waste Containment Technology Using a New Generation of Injectable Barrier Liquids*; Lawrence Berkeley National Lab.: Berkeley, CA, USA, 1996.
84. Moridis, G.J.; James, A.; Oldenburg, C. *Development of a Design Package for a Viscous Barrier at the Savannah River Site*; Lawrence Berkeley National Lab.: Berkeley, CA, USA, 1996.
85. Manchester, K.; Zaluski, M.; North-Abbott, M.; Trudnowski, J.; Bickford, J.; Wraith, J. Grout selection and characterization in support of the colloidal silica barrier deployment at Brookhaven National Laboratory. In Proceedings of the 2001 International Contain. and Remedies Technology Conference and Exhibition, Orlando, FL, USA, 10–13 June 2001.
86. Butrón, C. *Mechanical Behaviour of Silica Sol-Laboratory Studies Under Controlled Stress Conditions During the First Five Months of Hardening Process*; Department of Civil an Environmental Engineering, Division of GeoEngineering, Chalmers University of Technology: Goteborg, Sweden, 2005.
87. Butrón, C.; Axelsson, M.; Gustafson, G. Silica sol for rock grouting: Laboratory testing of strength, fracture behaviour and hydraulic conductivity. *Tunn. Undergr. Space Technol.* **2009**, *24*, 603–607. [CrossRef]
88. Shafigh, P.; Mahmud, H.B.; Jumaat, M.Z.; Zargar, M. Agricultural wastes as aggregate in concrete mixtures—A review. *Constr. Build. Mater.* **2014**, *53*, 110–117. [CrossRef]
89. Vik, E.A.; Sverdrup, L.; Kelley, A.; Storhaug, R.; Beitnes, A.; Boge, K.; Grepstad, G.K.; Tveiten, V. Experiences from environmental risk management of chemical grouting agents used during construction of the Romeriksporten tunnel. *Tunn. Undergr. Space Technol.* **2000**, *15*, 369–378. [CrossRef]
90. Gong, X. *The Manual of Ground Treatment*; China Architecture Publishing House: Beijing, China, 2008.
91. Holman, M. Nanomaterial forecast: Vols and Applications. In *ICON Nanomaterial Environmental Health and Safety Research Needs Assessment*; Lux Research: Amsterdam, The Netherland, 2007.